INTERNATIONAL JOURNAL OF
NUMERICAL ANALYSIS AND MODELING
Volume 15, Number 4-5, Pages 649–676

PENALTY-PROJECTION SCHEMES FOR THE CAHN-HILLIARD NAVIER-STOKES DIFFUSE INTERFACE MODEL OF TWO PHASE FLOW, AND THEIR CONNECTION TO DIVERGENCE-FREE COUPLED SCHEMES

LEO G. REBHOLZ, STEVEN M. WISE, AND MENGYING XIAO

(Communicated by M. Neda)

Dedicated to Professor William J. Layton on the occasion of his 60^{th} birthday

Abstract. We study and compare fully discrete numerical approximations for the Cahn-Hilliard-Navier-Stokes (CHNS) system of equations that enforce the divergence constraint in different ways, one method via penalization in a projection-type splitting scheme, and the other via strongly divergence-free elements in a fully coupled scheme. We prove a connection between these two approaches, and test the methods against standard ones with several numerical experiments. The tests reveal that CHNS system solutions can be efficiently and accurately computed with penalty-projection methods.

Key words. Cahn-Hilliard-Navier-Stokes system, penalty-projection method and strong divergence-free elements.

1. Introduction

The Cahn-Hilliard-Navier-Stokes (CHNS) system of equations is a diffuse interface model for the evolution of two-phase, immiscible, incompressible flows with uniform mass densities. In contrast to those of sharp interface type, the CHNS model describes a small-thickness transition region (diffuse interface) between the two immiscible fluids. This allows for convenient simulation of topological transitions such as pinch-off and reconnection of drops [25], without the need to explicitly track interfaces. In a domain $\Omega \subset \mathbb{R}^d$, d=2 or 3, with u representing velocity, p pressure, μ the chemical potential, and ϕ the phase field variable (taking a value of 1 in the bulk of one fluid and -1 in the bulk of the other), the CHNS system is given in non-dimensional form by [25]

$$\phi_t + \nabla \cdot (\phi u) = \nabla \cdot (M(\phi)\nabla \mu), \tag{1}$$

$$\mu = f_0'(\phi) - \epsilon^2 \Delta \phi, \tag{2}$$

$$u_t + u \cdot \nabla u + \nabla p - \nu \Delta u = -\frac{\epsilon^{-1}}{\mathrm{We}} \phi \nabla \mu, \tag{3}$$

$$\nabla \cdot u = 0, \tag{4}$$

together with initial conditions u_0 and ϕ_0, and boundary conditions

$$\begin{aligned} u|_{\partial\Omega} &= 0, \quad \text{(no slip, no penetration)}, \\ \nabla \phi \cdot n|_{\partial\Omega} &= 0, \quad \text{(local equilibrium)}, \\ \nabla \mu \cdot n|_{\partial\Omega} &= 0, \quad \text{(no flux)}. \end{aligned}$$

In the system above, ν is the kinematic viscosity ($\nu^{-1} = Re$, the Reynolds number), $\epsilon > 0$ is the transition layer width, We is a modified Weber number (measuring the

Received by the editors January 1, 2017 and, in revised form, April 24, 2017.
2000 *Mathematics Subject Classification.* 35K35,35Q35,65M12,75D06.

strength of the kinetic and surface energies [21]), $M(\phi)$ is the mobility function, which for simplicity we will take as $M(\phi) = 1$. The function $f_0(\phi) = \frac{1}{4}(1-\phi^2)^2 = \frac{1}{4}\phi^4 - \frac{1}{2}\phi^2 + \frac{1}{4}$ is the homogeneous free energy density function. We note that the energy balance of the system is easily shown to be

$$\frac{\partial}{\partial t}\left(\frac{1}{2}\|u\|^2 + \frac{\epsilon}{2\mathrm{We}}\|\nabla\phi\|^2 + \frac{\epsilon^{-1}}{\mathrm{We}}\int_\Omega f_0(\phi)\,dx\right) + \left(\nu\|\nabla u\|^2 + \frac{\epsilon^{-1}}{\mathrm{We}}\|\sqrt{M(\phi)}\nabla\mu\|^2\right) = 0.$$

By redefining the pressure, we can reformulate the system

$$\phi_t + \nabla\phi\cdot u = \nabla\cdot(M(\phi)\nabla\mu), \tag{5}$$

$$\mu = f_0'(\phi) - \epsilon^2\Delta\phi, \tag{6}$$

$$u_t + u\cdot\nabla u + \nabla p - \nu\Delta u = \frac{\epsilon^{-1}}{\mathrm{We}}\mu\nabla\phi, \tag{7}$$

$$\nabla\cdot u = 0. \tag{8}$$

Numerically solving the CHNS system is known to be very challenging for several reasons, including the fact that Navier-Stokes and Cahn-Hilliard equations can by themselves be difficult. For solutions to the coupled system, there are large spatial derivatives in the small transition regions causing stiff nonlinear systems. Moreover, the nonlinear algebraic equations resulting from discretization are large and strongly coupled, which makes it difficult to even 'get numbers' in a reasonable amount of time. Significant progress was recently made in [15], where a cleverly devised projection method was developed that decouples the pressure and divergence constraint from the system, but while still providing unconditional stability and (seemingly) second order temporal accuracy. Moreover, further decoupling of the system was done in the nonlinear iterations at each timestep, which further decoupled the system into easily solvable pieces. This scheme was shown to perform very well in terms of both accuracy and efficiency on a series of test problems.

The purpose of this paper is to study finite element schemes for (1)-(4) that more strongly enforce the divergence-constraint than what is usually found in the literature. In particular, we consider a coupled scheme that strongly enforces the divergence constraint, and a penalty-projection scheme that uses grad-div stabilization to better enforce the divergence constraint. Recent work in [10, 18, 22] has shown that the error caused in weak enforcement of the divergence constraint used by typical finite element methods for fluid simulations (e.g., using Taylor-Hood elements) is exacerbated when the momentum equation forcing has a large irrotational component [20]. Considering the CHNS system above, the forcing of the momentum equation (3) is observed to be either $-\frac{\epsilon^{-1}}{\mathrm{We}}\phi\nabla\mu$ or $\frac{\epsilon^{-1}}{\mathrm{We}}\mu\nabla\phi$, depending on the definition of the pressure. Since ϵ is small, we can expect the forcing to be large in general, especially in the diffuse interface region. Moreover, since $|\phi| \approx 1$ except in transition regions, we can expect the forcing the be nearly irrotational in bulk flow regions. Thus, the CHNS system seems to fit into a class of problems where stronger enforcement of the divergence constraint can significantly help solution accuracy.

There are many ways of reducing the effect of poor divergence-constraint enforcement in discretizations, including using point-wise divergence-free velocity-pressure elements (e.g., [20, 32, 2, 26, 13, 14, 8]) and using grad-div stabilization. Point-wise divergence-free elements completely eliminate the problem but come with difficulties such as larger (and discontinuous) pressure spaces, restrictive mesh conditions,

and the need to use higher order approximating polynomials degrees. Some of the more popular finite element software packages, like `deal.II` [3], do not support such elements. Grad-div stabilization, on the other hand, is easy to implement in most software packages, and significantly reduces the problem when the penalization parameter is chosen appropriately [18, 27, 28]. Moreover, grad-div stabilization can be easily incorporated into projection methods (which are then called penalty-projection methods [31]). Despite these differences, grad-div stabilization and point-wise divergence-free elements are closely related, and, in the recent paper [23], the authors proved that, in appropriate discrete settings, for simulations of single phase Navier-Stokes equations, penalty-projection methods with large stabilization parameters give almost identical approximations to point-wise divergence-free element solutions of coupled methods. In this paper, we will extend the ideas of [23] to schemes for the CHNS system.

This paper is arranged as follows. Section 2 presents notation and some mathematical preliminaries that will simplify the analysis to follows. Section 3 studies first order schemes, both coupled and projection, and proves that with certain meshes and element choices, the grad-div stabilized projection method will converge to the coupled method as the stabilization parameter goes to infinity. Section 4 extends the work of section 3 to second order schemes. Several numerical experiments are given that illustrate the theory, and show the effectiveness of the grad-div stabilized projection method with large stabilization parameter. Finally, conclusions are drawn in section 5.

2. Notation and Mathematical Prelimilaries

We consider an open, bounded, polygonal domain $\Omega \subset \mathbb{R}^d$, $d = 2$ or 3, and denote the usual $L^2(\Omega)$ norm and inner product by $\|\cdot\|$ and $(\cdot,\cdot)$, respectively. All other norms and inner products will be clearly labeled. For any $\psi \in L^2(\Omega)$, define the spatial average $\overline{\psi} := |\Omega|^{-1}\int_\Omega \psi\, dx$. We will use the following function spaces:

$$\begin{aligned} S &:= H^1(\Omega), \\ X &:= [H_0^1(\Omega)]^d = \left\{ v \in [H^1(\Omega)]^d \;\middle|\; v|_{\partial\Omega} = 0 \right\}, \\ Q &:= L_0^2(\Omega) = \left\{ q \in L^2(\Omega) \;\middle|\; \overline{q} = 0 \right\}. \end{aligned}$$

Recall that in X, the Poincaré inequality holds: there exists $C = C(\Omega) > 0$ such that

$$\|v\| \le C\|\nabla v\|, \quad \forall\, v \in X.$$

This allows us to define $(u,v)_X := (\nabla u, \nabla v)$ as the inner product on X, and $\|u\|_X := \|\nabla u\|$ as the associated norm. We set $\mathring{H}^1(\Omega) = H^1(\Omega) \cap L_0^2(\Omega)$. Since (weak and strong) solutions of the Cahn-Hilliard equation are mass conservative, that is, $d_t \int_\Omega \phi \; dx = 0$, we have $\phi(t) \in \mathring{H}^1(\Omega) + \overline{\phi}_0$, for all $t \ge 0$. For any $\psi \in \mathring{H}^1(\Omega) + \overline{\phi}_0$, there is a constant $C = C(\Omega) > 0$, such that,

$$\|\psi\| = \left\|\psi - \overline{\phi}_0 + \overline{\phi}_0\right\| \le \left\|\psi - \overline{\phi}_0\right\| + \|\overline{\phi}_0\| \le C\|\nabla\psi\| + \sqrt{|\Omega|}\cdot|\overline{\phi}_0|.$$

We will also use the function space

$$Y := \left\{ v \in L^2(\Omega) \;\middle|\; \nabla\cdot v \in L^2(\Omega) \text{ and } v\cdot n\,|_{\partial\Omega} = 0 \right\}$$

for the projection-type scheme analysis. Observe that $X \subset Y$.

2.1. Discretization preliminaries. Let $\mathcal{T}_h = \{K\}$ be a conforming triangulation of Ω, and define

$$P_r^\diamond := \left\{ v \in L^2(\Omega) \;\middle|\; v_K \in \mathcal{P}_r,\ \forall K \in \mathcal{T}_h \right\}, \quad P_r := P_r^\diamond \cap C^0(\overline{\Omega}).$$

Note that $P_r^\diamond$ is the "broken" piece-wise polynomial space. We consider discrete subspaces for the phase variable $S_h \subset S$; the chemical potential, $W_h \subset S$; the velocity, $X_h \subset X$; and the pressure, $Q_h \subset Q$. For simplicity, we will take $S_h = W_h = P_k$. This choice will facilitate the higher-order estimates that we will seek for the Cahn-Hilliard discretization [6, 7, 9]. We want the pair (X_h, Q_h) to satisfy the LBB condition,

$$\inf_{q\in Q_h} \sup_{v\in X_h} \frac{(\nabla\cdot v, q)}{\|q\|\|\nabla v\|} \geq \beta > 0.$$

Herein, we will consider Taylor-Hood elements,

$$(X_h, Q_h) = ([P_k]^d \cap X, P_{k-1} \cap Q),\ 2 \leq k, \quad \text{(Taylor-Hood)},$$

and Scott-Vogelius elements

$$(X_h, Q_h) = ([P_k]^d \cap X, P_{k-1}^\diamond \cap Q),\ 2 \leq k \leq d, \quad \text{(Scott-Vogelius)},$$

both of which are known to be LBB stable. Scott-Vogelius elements have the added property that $\nabla \cdot X_h \subset Q_h$, which leads to a strong enforcement of the divergence constraint. We will be clear when we assume that $\nabla\cdot X_h \subset Q_h$. For LBB to hold, Scott-Vogelius elements require restrictions on the mesh and polynomial degrees, the least restrictive of which are that the meshes be created as barycenter refinements of regular triangulations/tetrahedralizations and that $k \leq d$ [2, 32].

For the projection-type scheme, we will also utilize the space $Y_h \subset Y$, $Y_h = [P_k]^d \cap Y$. The polynomial degree k used for Y_h will be the same as for X_h. Since $X_h \subset Y_h$, if the LBB condition holds for (X_h, Q_h), it must also hold for (Y_h, Q_h). Indeed, for any $q \in Q_h$,

$$\sup_{v\in Y_h} \frac{(\nabla\cdot v, q)}{\|\nabla v\|} \geq \sup_{v\in X_h} \frac{(\nabla\cdot v, q)}{\|\nabla v\|} \geq \beta\|q\|.$$

Moreover, if $Q_h = P_{k-1}^\diamond \cap Q$, then $\nabla \cdot Y_h \subset Q_h$ holds since $\nabla \cdot [P_k]^d \subset P_{k-1}^\diamond$, and functions in $\{\nabla \cdot Y_h\}$ must have zero mean due the no penetration boundary condition in Y_h and the divergence theorem. Thus, since we require the same polynomial degree for X_h and Y_h, for this choice of pressure space we have that $\nabla \cdot X_h \subset \nabla \cdot Y_h \subset Q_h$.

Define the discrete weakly divergence-free subspace, V_h, via

$$V_h := \{v \in X_h \mid (\nabla \cdot v, q) = 0,\ \forall\ q \in Q_h\}.$$

For the Scott-Vogelius elements, $\nabla\cdot X_h \subset Q_h$ and, consequently, the discrete weakly divergence-free space is identical to the point-wise divergence-free space in the sense that

$$V_h = \{v \in X_h \mid \|\nabla \cdot v\| = 0\}.$$

Define

$$R_h := V_h^\perp = \{v \in X_h \mid (\nabla v, \nabla w) = 0,\ \forall w \in V_h\ \},$$

the orthogonal complement of V_h with respect to the X inner product. Thus $X_h = V_h \oplus R_h$. The following lemma from [23] proves the equivalence of the L^2 divergence norm and X-norm in R_h:

Lemma 2.1. *Suppose $(X_h, Q_h) \subset (X, Q)$ satisfies the inf-sup condition, $\nabla \cdot X_h \subset Q_h$, and $X_h = V_h \oplus R_h$, where $R_h = V_h^{\perp}$, as above. Then we have*

$$\|\nabla v_h\| \leq C_R \|\nabla \cdot v_h\|, \qquad \forall v_h \in R_h,$$

where C_R is a constant independent of h.

Define the skew-symmetric, trilinear operator $B_0 : X \times X \times X \to \mathbb{R}$ by

$$B_0(u, v, w) := \frac{1}{2}(u \cdot \nabla v, w) - \frac{1}{2}(u \cdot \nabla w, v)$$

and recall, from e.g. [11], that there exists C_s depending on Ω such that

$$|B_0(u, v, w)| \leq C_s \|u\|^{1/2} \|\nabla u\|^{1/2} \|\nabla v\| \|\nabla w\|,$$

for every $u, v, w \in X$.

For the next few estimates, we need the discrete Laplacian, $\Delta_h : S_h \to \mathring{S}_h := S_h \cap L_0^2(\Omega)$, which is defined as follows: for any $\phi_h \in S_h$, $\Delta_h \phi_h \in \mathring{S}_h$ denotes the unique solution to the problem

$$(\Delta_h \phi_h, \chi) = -(\nabla \phi_h, \nabla \chi), \quad \forall\, \chi \in S_h. \tag{9}$$

Some of its properties can be found in [24]. We make important use of the following discrete Sobolev inequalities [17, 24]:

Proposition 2.1. *If Ω is a convex polygonal domain in $\mathbb{R}^d$, $d = 2, 3$, and $\mathcal{T}_h$ is a globally quasi-uniform family of triangulations of Ω, then for all $\psi_h \in S_h$,*

$$\|\psi_h\|_{L^\infty} \leq C \|\Delta_h \psi_h\|^{\frac{d}{2(6-d)}} \|\psi_h\|_{L^6}^{\frac{3(4-d)}{2(6-d)}} + C \|\psi_h\|_{L^6}, \tag{10}$$

$$\|\nabla \psi_h\|_{L^4} \leq C \|\Delta_h \psi_h\|^{\frac{d}{4}} \|\nabla \psi_h\|^{\frac{4-d}{4}} + C \|\nabla \psi_h\|, \tag{11}$$

$$\|\nabla \psi_h\|_{L^6} \leq C \|\Delta_h \psi_h\| + C \|\nabla \psi_h\|. \tag{12}$$

for some constant $C > 0$ that is independent of h.

Here we define two different convection coupling trilinear forms:

$$B_1(\psi, v, \chi) := (\nabla \psi \cdot v, \chi), \tag{13}$$

$$B_2(\psi, v, \chi) := (\nabla \psi \cdot v, \chi) + (\nabla \cdot v, \psi \chi). \tag{14}$$

The B_1 trilinear form is commonly used in Cahn-Hilliard type schemes [6, 7], however, it only allows for mass conservation if the pressure and phase spaces are the same. The B_2 form is more flexible, allowing for mass conservation even when choosing different pressure and phase spaces. We give bounds for both forms, as even though we use B_2 exclusively in this work. We show here that the upper bounds are the same for B_1 and B_2, which will allow us to invoke known theory from similar works which use the B_1 trilinear form. We have the following mass conservation properties and estimates for these trilinear forms.

Proposition 2.2. *Assume that S_h, X_h, Q_h, and V_h are defined as above, but that $\nabla \cdot X_h \subset Q_h$ does not necessarily hold.*

(1) *If $\psi_h \in S_h \cap Q_h$ and $v_h \in V_h$, then*

$$B_1(\psi_h, v_h, 1) = 0.$$

(2) *If $\psi_h \in S_h$, $v_h \in V_h$ are arbitrary, then*

$$B_2(\psi_h, v_h, 1) = 0.$$

(3) *If* $\psi_h \in S_h \cap Q_h$, $\chi_h \in S_h$, *and* $v_h \in V_h$, *then*

$$|B_1(\psi_h, v_h, \chi_h)| \leq C\|\nabla\psi_h\| \cdot \|\nabla v_h\| \cdot \|\nabla\chi_h\|,$$

and if $\psi_h, \chi_h \in S_h$, *and* $v_h \in V_h$, *then*

$$|B_2(\psi_h, v_h, \chi_h)| \leq C\left(\|\nabla\psi_h\| + |\overline{\psi_h}|\right) \cdot \|\nabla v_h\| \cdot \|\nabla\chi_h\|.$$

(4) *If* $\psi_h \in S_h \cap Q_h$, $\chi_h \in S_h$, *and* $v_h \in X_h$, *then*

$$|B_1(\psi_h, v_h, \chi_h)| \leq C\|\nabla\psi_h\| \cdot \|\nabla v_h\| \cdot \|\chi_h\|_{H^1},$$

and if $\psi_h, \chi_h \in S_h$, *and* $v_h \in X_h$, *then*

$$|B_2(\psi_h, v_h, \chi_h)| \leq C\left(\|\nabla\psi_h\| + |\overline{\psi_h}|\right) \cdot \|\nabla v_h\| \cdot \|\chi_h\|_{H^1}.$$

(5) *If* $\psi_h, \chi_h \in S_h$, $v_h \in X_h$ *and* Ω *is a convex, polygonal domain, then*

$$|B_1(\psi_h, v_h, \chi_h)| \leq C\left(\|\Delta_h\psi_h\| + \|\nabla\psi_h\|\right) \cdot \|\nabla v_h\| \cdot \|\chi_h\|,$$

and

$$|B_2(\psi_h, v_h, \chi_h)| \leq C\left(\|\Delta_h\psi_h\| + \|\nabla\psi_h\| + \left|\overline{\psi}_h\right|\right) \cdot \|\nabla v_h\| \cdot \|\chi_h\|.$$

Proof. (1) If $\psi_h \in S_h \cap Q_h$ and $v_h \in V_h$, then using Green's theorem, the property that $v_h|_{\partial\Omega} = 0$ and the discrete weak divergence-free property of V_h, we obtain

$$B_1(\psi_h, v_h, 1) = (\nabla\psi_h, v_h) = -(\psi_h, \nabla \cdot v_h) + (\psi_h, v_h \cdot n)_{\partial\Omega} = 0.$$

(2) If $\psi_h \in S_h$, $v_h \in V_h$, then again using Green's theorem and the property that $v_h|_{\partial\Omega} = 0$ (but *not* the discrete weak divergence-free property of V_h), we get that

(15)
$$B_2(\psi_h, v_h, 1) = (\nabla\psi_h, v_h) + (\nabla\cdot v_h, \psi_h) = -(\psi_h, \nabla\cdot v_h) + (\psi_h, v_h\cdot n)_{\partial\Omega} + (\nabla\cdot v_h, \psi_h) = 0.$$

(3) Suppose $\psi_h \in S_h \cap Q_h$,$\chi_h \in S_h$ and $v_h \in V_h$. By part (a),

$$B_1(\psi_h, v_h, \chi_h) = B_1(\psi_h, v_h, \chi_h - \overline{\chi_h}).$$

Using Hölder's inequality, the Sobolev embedding $H^1(\Omega) \hookrightarrow L^4(\Omega)$, and the appropriate Poincaré inequalities, we have

$$|B_1(\psi_h, v_h, \chi_h)| \leq \|\nabla\psi_h\| \cdot \|v_h\|_{L^4} \cdot \|\chi_h - \overline{\chi_h}\|_{L^4} \leq C\|\nabla\psi_h\| \cdot \|\nabla v_h\| \cdot \|\nabla\chi_h\|.$$

Next, suppose $\psi_h, \chi_h \in S_h$ (*i.e.*, $\psi_h \in Q_h$ need not hold) and $v_h \in V_h$. By part (2),

$$B_2(\psi_h, v_h, \chi_h) = B_2(\psi_h, v_h, \chi_h - \overline{\chi_h}).$$

Using Hölder's inequality, the Sobolev embedding $H^1(\Omega) \hookrightarrow L^4(\Omega)$, and the appropriate Poincaré inequalities, we have

$$\begin{aligned}|B_2(\psi_h, v_h, \chi_h)| &\leq \|\nabla\psi_h\| \cdot \|v_h\|_{L^4} \cdot \|\chi_h - \overline{\chi_h}\|_{L^4} + C\|\psi_h\|_{L^4} \cdot \|\nabla v_h\| \cdot \|\chi_h - \overline{\chi_h}\|_{L^4} \\ &\leq C\left(\|\nabla\psi_h\| + |\overline{\psi_h}|\right) \cdot \|\nabla v_h\| \cdot \|\nabla\chi_h\|.\end{aligned}$$

(4) This case is similar to (3), except that we can't invoke (1) or (2), since $v_h \notin V_h$.

(5) Finally, suppose $\psi_h, \chi_h \in S_h$, $v_h \in X_h$. Then using Hölder's inequality, the Sobolev embeddings $H^1(\Omega) \hookrightarrow L^4(\Omega)$ and $H^1(\Omega) \hookrightarrow L^6(\Omega)$, the Poincaré inequalities

$$\|\phi_h\| \leq C\left(\|\nabla\phi_h\| + \left|\overline{\phi_h}\right|\right), \quad \|\nabla\phi_h\| \leq C\|\Delta_h\phi_h\|, \quad \text{for all } \phi_h \in S_h,$$

and the estimates (10) and (11), we have

$$\begin{aligned}|B_2(\psi_h, v_h, \chi_h)| &\le \|\nabla\psi_h\|_{L^4} \cdot \|v_h\|_{L^4} \cdot \|\chi_h\| + C\|\psi_h\|_{L^\infty} \cdot \|\nabla v_h\| \cdot \|\chi_h\| \\ &\le C\left((\|\nabla\psi_h\| + \|\Delta_h\psi_h\|)^{\frac{d}{4}} \|\nabla\psi_h\|^{\frac{4-d}{4}}\right) \cdot \|\nabla v_h\| \cdot \|\chi_h\| \\ &\quad + C\left(\|\Delta_h\psi_h\|^{\frac{d}{2(6-d)}} \|\psi_h\|_{L^6}^{\frac{3(4-d)}{2(6-d)}} + C\|\psi_h\|_{L^6}\right) \cdot \|\nabla v_h\| \cdot \|\chi_h\| \\ &\le C\left(\|\Delta_h\psi_h\| + \|\nabla\psi_h\| + \left|\overline{\psi_h}\right|\right) \cdot \|\nabla v_h\| \cdot \|\chi_h\|.\end{aligned}$$

The estimate for B_1 is similar. □

We will use the following discrete Gronwall inequality in our analysis [16].

Lemma 2.2. *(Discrete Gronwall Lemma). Let $\Delta t, H,$ and a_n, b_n, c_n, d_n (for intergers $n \ge 0$) be non-negative numbers such that*

$$a_l + \Delta t \sum_{n=0}^{l} b_n \le \Delta t \sum_{n=0}^{l} d_n a_n + \Delta t \sum_{n=0}^{l} c_n + H \quad \text{for } l \ge 0,$$

If $\Delta t d_n < 1\ \forall n$, then

$$a_l + \Delta t \sum_{n=0}^{l} b_n \le \exp\left(\Delta t \sum_{n=0}^{l} \frac{d_n}{1 - \Delta t d_n}\right)\left(\Delta t \sum_{n=0}^{l} c_n + H\right).$$

3. First order schemes for Cahn-Hilliard-Navier-Stokes

We will study, test, and show connections between first order coupled and penalty-projection schemes for CHNS system. We present these schemes now.

3.1. A first order coupled scheme for CHNS system.

Algorithm 3.1. *(Coupled scheme for CHNS system) Given parameters ϵ,* We, *ν, and Δt, find*

$$(\hat{\phi}_h^{n+1}, \hat{\mu}_h^{n+1}, \hat{u}_h^{n+1}, \hat{p}_h^{n+1}) \in (S_h, S_h, X_h, Q_h)$$

satisfying for all $(\chi_h, \psi_h, v_h, q_h) \in (S_h, S_h, X_h, Q_h)$,

$$\begin{aligned}\frac{1}{\Delta t}\left(\hat{\phi}_h^{n+1} - \hat{\phi}_h^n, \chi_h\right) + B_2\left(\hat{\phi}_h^n, \hat{u}_h^{n+1}, \chi_h\right) + (\nabla\hat{\mu}_h^{n+1}, \nabla\chi_h) &= 0, \\ (\hat{\mu}_h^{n+1}, \psi_h) - ((\hat{\phi}_h^{n+1})^3, \psi_h) + (\hat{\phi}_h^n, \psi_h) - \epsilon^2(\nabla\hat{\phi}_h^{n+1}, \nabla\psi_h) &= 0, \\ \frac{1}{\Delta t}(\hat{u}_h^{n+1} - \hat{u}_h^n, v_h) + \nu(\nabla\hat{u}_h^{n+1}, \nabla v_h) + B_0(\hat{u}_h^n, \hat{u}_h^{n+1}, v_h) & \\ -(\hat{p}_h^{n+1}, \nabla\cdot v_h) - \frac{\epsilon^{-1}}{\mathrm{We}} B_2\left(\hat{\phi}_h^n, v_h, \hat{\mu}_h^{n+1}\right) &= 0, \\ (\nabla\cdot\hat{u}_h^{n+1}, q_h) &= 0,\end{aligned}$$

for $0 \le k \le L-1$, where $L = \frac{T}{\Delta t}$.

Following [6, 7], we can prove unconditional unique solvability, unconditional energy stability, unconditional $\ell^\infty(0, T; L^\infty)$ stability for $\hat{\phi}_h$, and convergence for this scheme. In particular, we can derive optimal-order error estimates for the variables in the appropriate energy norms.

Lemma 3.1. *Suppose $(X_h, Q_h) \subset (X, Q)$ satisfies the inf-sup condition, $\nabla \cdot X_h \subset Q_h$, and $u_h^0 \in V_h$ and $\phi_h^0 \in S_h$. Then Algorithm 3.1 is uniquely solvable, and its solutions satisfy*

$$\|\hat{u}_h^L\|^2 + \|\nabla\hat{\phi}_h^L\|^2 + \|\Delta_h\hat{\phi}_h^L\|^2 + \|\hat{\phi}_h^L\|_{L^\infty}^2 + \Delta t\sum_{n=1}^{L}\left(\|\nabla\hat{u}_h^n\|^2 + \gamma\|\nabla\cdot\hat{u}_h^n\|^2 + \|\hat{\mu}_h^n\|_{H^1}^2\right) \leq C(data), \tag{16}$$

where C depends on problem data, but is independent of h and Δt. Moreover, if we assume that $X_h = X \cap [P_k]^d$, $Q_h = Q \cap P_{k-1}^\diamond$, $S_h = P_k$, and (u, p, ϕ, μ) is a sufficiently regular, strong CHNS system solution, then

$$\|\hat{u}_h^L - u(T)\|^2 + \|\nabla(\hat{\phi}_h^L - \phi(T))\|^2 + \Delta t\sum_{n=1}^{L}\left(\|\nabla(\hat{u}_h^n - u(t^n))\|^2 + \|\hat{\mu}_h^n - \mu(t^n)\|_{H^1}^2\right) \leq C(\Delta t^2 + h^{2k}), \tag{17}$$

with C dependent on problem data, but is independent of h and Δt.

Remark 3.1. *Observe that the term $\gamma\|\nabla\cdot\hat{u}_h^n\|^2$ in estimate* (16) *is identically zero.*

Remark 3.2. *The stability bound on $\|\hat{\phi}_h\|_{\ell^\infty(H^1)}$ depends linearly on ϵ^{-2}, and comes directly from the energy stability of the method and our particular scaling of the energy. The scaling in* [6, 9] *yields a dependence of ϵ^{-1}. The higher order stability estimates may depend linearly on ϵ^{-m} for small and modestly-sized positive integer values m. Hence the estimates are singular with respect to ϵ. We do not track this dependence upon ϵ here, but see* [9] *for a related discussion where the dependences are more carefully tracked.*

Proof of Lemma 3.1. The proofs of unique solvability, stability and convergence are long and technical, however, they follow analogously to the results for the second-order coupled scheme for CHNS system studied in [7] and first-order coupled scheme for the Cahn-Hilliard-Stokes system studied in [6]. Thus, we omit the proofs, with the exception of those concerning stability, since the tools used therein will be used in later results in this paper.

The stability proof begins with an energy-type stability estimate. Later steps in the proof will be used to gain regularity. The constants involved in the regularity upper bounds will be independent of h and Δt.

Step 1: $\hat{u}_h \in \ell^2(0,T;H^1)\cap\ell^\infty(0,T;L^2)$, $\hat{\phi}_h \in \ell^\infty(0,T;H^1)$, and $\nabla\hat{\mu}_h \in \ell^2(0,T;L^2)$.

We begin the proof by picking test functions $v_h = \epsilon \mathrm{We}\Delta t \hat{u}_h^{n+1}$, $\chi_h = \Delta t \hat{\mu}_h^{n+1}$, $q_h = \hat{p}_h^{n+1}$, $\psi_h = \hat{\phi}_h^{n+1} - \hat{\phi}_h^n$. This gives

$$\begin{aligned}
\left(\hat{\phi}_h^{n+1} - \hat{\phi}_h^n, \mu_h^{n+1}\right) + \Delta t B_2\left(\hat{\phi}_h^n, \hat{u}_h^{n+1}, \mu_h^{n+1}\right) + \Delta t \|\nabla \hat{\mu}_h^{n+1}\|^2 &= 0, \\
\frac{\epsilon^2}{2}\left(\|\nabla \hat{\phi}_h^{n+1}\|^2 - \|\nabla \hat{\phi}_h^n\|^2 + \|\nabla(\hat{\phi}_h^{n+1} - \hat{\phi}_h^n)\|^2\right) & \\
-(\hat{\mu}_h^{n+1}, \hat{\phi}_h^{n+1} - \hat{\phi}_h^n) + ((\hat{\phi}_h^{n+1})^3, \hat{\phi}_h^{n+1} - \hat{\phi}_h^n) - (\hat{\phi}_h^n, \hat{\phi}_h^{n+1} - \hat{\phi}_h^n) &= 0, \\
\frac{\epsilon \mathrm{We}}{2}\left(\|\hat{u}_h^{n+1}\|^2 - \|\hat{u}_h^n\|^2 + \|\hat{u}_h^{n+1} - \hat{u}_h^n\|^2\right) + \epsilon \mathrm{We}\nu\Delta t \|\nabla \hat{u}_h^{n+1}\|^2 & \\
-\Delta t B_2\left(\hat{\phi}_h^n, \hat{u}_h^{n+1}, \hat{\mu}_h^{n+1}\right) &= 0,
\end{aligned}$$

noting that the B_0 term dropped due to the skew-symmetry property, and the pressure term dropped thanks to the discrete mass conservation property. Next, we add the equations together, and note the cancellation of the B_2 and $(\hat{\mu}_h^{n+1}, \hat{\phi}_h^{n+1} - \hat{\phi}_h^n)$ terms. This yields the equation

$$\begin{aligned}
&\frac{\epsilon^2}{2}\left(\|\nabla \hat{\phi}_h^{n+1}\|^2 - \|\nabla \hat{\phi}_h^n\|^2 + \|\nabla(\hat{\phi}_h^{n+1} - \hat{\phi}_h^n)\|^2\right) \\
&\quad + \frac{\epsilon \mathrm{We}}{2}\left(\|\hat{u}_h^{n+1}\|^2 - \|\hat{u}_h^n\|^2 + \|\hat{u}_h^{n+1} - \hat{u}_h^n\|^2\right) + \epsilon \mathrm{We}\nu\Delta t \|\nabla \hat{u}_h^{n+1}\|^2 \\
&\qquad + \Delta t \|\nabla \hat{\mu}_h^{n+1}\|^2 + ((\hat{\phi}_h^{n+1})^3 - \hat{\phi}_h^n, \hat{\phi}_h^{n+1} - \hat{\phi}_h^n) = 0.
\end{aligned} \tag{18}$$

From [6], we have an identity for the last term in (18),

$$\begin{aligned}
&((\hat{\phi}_h^{n+1})^3 - \hat{\phi}_h^n, \hat{\phi}_h^{n+1} - \hat{\phi}_h^n) \\
= \;& \frac{1}{4}\left(\|(\hat{\phi}_h^{n+1})^2 - 1\|^2 - \|(\hat{\phi}_h^n)^2 - 1\|^2 + \|(\hat{\phi}_h^{n+1})^2 - (\hat{\phi}_h^n)^2\|^2\right) \\
&+ \frac{1}{2}\left(\|\hat{\phi}_h^{n+1}(\hat{\phi}_h^{n+1} - \hat{\phi}_h^n)\|^2 + \|\hat{\phi}_h^{n+1} - \hat{\phi}_h^n\|^2\right).
\end{aligned}$$

Defining $E(u, \phi) := \frac{\epsilon \mathrm{We}}{2}\|u\|^2 + \frac{\epsilon^2}{2}\|\nabla \phi\|^2 + \|\phi^2 - 1\|^2$, we can reduce (18) with the above identity and dropping positive terms on the left hand side to obtain the bound

$$E(\hat{u}_h^{n+1}, \hat{\phi}_h^{n+1}) - E(\hat{u}_h^n, \hat{\phi}_h^n) + \epsilon \mathrm{We}\nu\Delta t \|\nabla \hat{u}_h^{n+1}\|^2 + \Delta t \|\nabla \hat{\mu}_h^{n+1}\|^2 \le 0. \tag{19}$$

Summing over time steps gives the bound

$$E(\hat{u}_h^L, \hat{\phi}_h^L) + \epsilon \mathrm{We}\nu\Delta t \sum_{n=1}^{L} \|\nabla \hat{u}_h^n\|^2 + \Delta t \sum_{n=1}^{L} \|\nabla \hat{\mu}_h^n\|^2 \le E(\hat{u}_h^0, \hat{\phi}_h^0),$$

which implies the stated results for $\hat{u}_h$ and $\nabla \hat{\mu}_h$, since $\hat{u}_h^0 \in L^2(\Omega)$ and $\hat{\phi}_h^0 \in H^1(\Omega)$. For $\hat{\phi}_h$ we have, for any $0 \le n \le L$,

$$\epsilon^2 \|\nabla \hat{\phi}_h^n\|^2 \le E(\hat{u}_h^n, \hat{\phi}_h^n) \le E(\hat{u}_h^0, \hat{\phi}_h^0) \le C.$$

Furthermore, since the scheme conserves mass, that is, $\overline{\hat{\phi}_h^n} = \overline{\hat{\phi}_h^0}$, we observe that

$$\|\hat{\phi}_h^n\| \le \|\hat{\phi}_h^n - \overline{\hat{\phi}_h^n}\| + \|\overline{\hat{\phi}_h^n}\| \le C\|\nabla \hat{\phi}_h^n\| + \sqrt{|\Omega|}\left|\overline{\hat{\phi}_h^0}\right| \le C,$$

for all $0 \le n \le L$. Therefore, $\|\hat{\phi}_h^n\|_{H^1} \le C$, for all $0 \le n \le L$.

Step 2: $\Delta_h \hat{\phi}_h \in \ell^2(0, T; L^2)$.

Next, choose $\psi_h = \Delta_h \hat{\phi}_h^{n+1}$ in Algorithm 3.1, then use properties of the discrete Laplacian, then Cauchy-Schwarz and Young's inequalities to obtain

$$\begin{aligned}\epsilon^2\|\Delta_h\hat{\phi}_h^{n+1}\|^2 &= (\nabla\hat{\mu}_h^{n+1}, \nabla\hat{\phi}_h^{n+1}) + ((\hat{\phi}_h^{n+1})^3 - \hat{\phi}_h^n, \Delta_h\hat{\phi}_h^{n+1}) \\ &\leq \frac{1}{2}\|\nabla\hat{\mu}_h^{n+1}\|^2 + \frac{1}{2}\|\nabla\hat{\phi}_h^{n+1}\|^2 + \frac{1}{2\epsilon^2}\|(\hat{\phi}_h^{n+1})^3 - \hat{\phi}_h^n\|^2 + \frac{\epsilon^2}{2}\|\Delta_h\hat{\phi}_h^{n+1}\|^2.\end{aligned}$$

From the regularity of $\hat{\phi}_h$ already established, we have that

$$\|(\hat{\phi}_h^{n+1})^3 - \hat{\phi}_h^n\|^2 \leq 2\|\hat{\phi}_h^{n+1}\|_{L^6}^6 + 2\|\hat{\phi}_h^n\|^2 \leq C(\|\hat{\phi}_h^{n+1}\|_{H^1}^6 + \|\hat{\phi}_h^n\|^2) \leq C,$$

and thus

$$\epsilon^2\|\Delta_h\hat{\phi}_h^{n+1}\|^2 \leq \|\nabla\hat{\mu}_h^{n+1}\|^2 + C.$$

Multiplying both sides by Δt, summing over time steps, and using that $\nabla\hat{\mu}_h \in \ell^2(0,T;L^2)$ proves the Step 2 result.

Step 3: $\hat{\mu}_h \in \ell^2(0,T;H^1)$.

It is already established in Step 1 that $\nabla\hat{\mu}_h \in \ell^2(0,T;L^2)$, and so it remains to show $\hat{\mu}_h \in \ell^2(0,T;L^2)$. Choose the test function $\psi_h = \mu_h^{n+1}$ in Algorithm 3.1 to obtain the equation

$$\|\hat{\mu}_h^{n+1}\|^2 = ((\hat{\phi}_h^{n+1})^3 - \hat{\phi}_h^n, \hat{\mu}_h^{n+1}) + \epsilon^2(\nabla\hat{\phi}_h^{n+1}, \nabla\hat{\mu}_h^{n+1}).$$

Using Cauchy-Schwarz and Young's inequalities, the bound on the nonlinear term from Step 2, and the regularity of $\hat{\phi}_h$ proven in Step 1 yields

$$\begin{aligned}\|\hat{\mu}_h^{n+1}\|^2 &\leq \|(\hat{\phi}_h^{n+1})^3 - \hat{\phi}_h^n\|^2 + \epsilon^2\|\nabla\hat{\phi}_h^{n+1}\|^2 + \|\nabla\hat{\mu}_h^{n+1}\|^2 \\ &\leq C + \|\nabla\hat{\mu}_h^{n+1}\|^2.\end{aligned}$$

Now multiplying both sides by Δt, summing over time steps, and using the regularity of $\nabla\hat{\mu}_h$ proven in Step 1 provide the Step 3 result.

Step 4: $\Delta_h\hat{\phi}_h \in \ell^\infty(0,T;L^2)$ and $\hat{\phi}_h \in \ell^\infty(0,T;L^\infty)$.

This step follows as in [6, 7]. The details are tedious and are skipped for the sake of brevity. □

3.2. A penalty-projection scheme for the Cahn-Hilliard-Navier-Stokes system. We also consider herein a projection method for CHNS system. The scheme is an analogue to the projection method for the NSE: implicit pressure is removed from the coupled system, and is recovered in an additional step that uses a Hodge decomposition to break the velocity into a divergence-free part and a potential part. The pressure is defined as the potential part.

Projection methods are known to be more efficient than coupled methods, since their two steps are generally much easier to solve than the one step needed in coupled methods. However, they are also known to be less accurate in general (although there are many 'fixes' available for various settings). One method that can provide significant improvement is to add grad-div stabilization to the method to penalize divergence error in step 1 of the projection method. When this is done, the methods are often called 'penalty-projection', and are well studied for Navier-Stokes equations [1, 4, 19, 23, 30].

The penalty-projection scheme we consider is the one associated with the coupled scheme in Algorithm 3.1, and is stated below.

Algorithm 3.2. *(Penalty-projection scheme for CHNS system) Given parameters* ϵ, We, ν, *and* Δt,

Step 1: Find $(\phi_h^{n+1}, \mu_h^{n+1}, u_h^{n+1}) \in (S_h, S_h, X_h)$ *satisfying for all* $(\chi_h, \psi_h, v_h) \in (S_h, S_h, X_h)$,

$$\begin{aligned}
\frac{1}{\Delta t}\left(\phi_h^{n+1} - \phi_h^n, \chi_h\right) + B_2\left(\phi_h^n, u_h^{n+1}, \chi_h\right) + (\nabla \mu_h^{n+1}, \nabla \chi_h) &= 0,\\
(\mu_h^{n+1}, \psi_h) - ((\phi_h^{n+1})^3, \psi_h) + (\phi_h^n, \psi_h) - \epsilon^2(\nabla \phi_h^{n+1}, \nabla \psi_h) &= 0,\\
\frac{1}{\Delta t}(u_h^{n+1} - \bar{u}_h^n, v_h) + \gamma(\nabla \cdot u_h^{n+1}, \nabla \cdot v_h) + \nu(\nabla u_h^{n+1}, \nabla v_h)&\\
+B_0(u_h^n, u_h^{n+1}, v_h) - \frac{\epsilon^{-1}}{\mathrm{We}} B_2\left(\phi_h^n, v_h, \mu_h^{n+1}\right) &= 0.
\end{aligned}$$

Step 2: Find $(\bar{u}_h^{n+1}, p_h^{n+1}) \in (Y_h, Q_h)$ *such that for every* $(v_h, q_h) \in (Y_h, Q_h)$

$$\begin{aligned}
\frac{1}{\Delta t}(\bar{u}_h^{n+1} - u_h^{n+1}, v_h) - (p_h^{n+1}, \nabla \cdot v_h) &= 0,\\
(\nabla \cdot \bar{u}_h^{n+1}, q_h) &= 0.
\end{aligned}$$

Remark 3.3. *Observe that* $X_h \subset Y_h$, *and if* $\nabla \cdot Y_h \subset Q_h$ *(as it is if* $Q_h = P_{k-1}^{\diamond} \cap Q$ *and* $Y_h = [P_k]^d \cap Y$*), then* $\|\nabla \cdot \bar{u}_h^{n+1}\| = 0$.

The penalty-projection scheme above is both uniquely solvable, and unconditionally stable.

Lemma 3.2. *Suppose* $(X_h, Q_h) \subset (X, Q)$ *satisfies the inf-sup condition,* $\nabla \cdot X_h \subset \nabla \cdot Y_h \subset Q_h$, *and* $u_h^0 \in V_h$ *and* $\phi_h^0 \in S_h$. *Then Algorithm 3.2 is uniquely solvable, and its solution satifies*

(20)
$$\|u_h^L\|^2 + \|\nabla \phi_h^L\|^2 + \|\Delta_h \phi_h^L\| + \|\phi_h^L\|_{L^\infty}^2 + \Delta t \sum_{n=1}^{L} \left(\|\nabla u_h^n\|^2 + \gamma \|\nabla \cdot u_h^n\|^2 + \|\mu_h^n\|_{H^1}^2\right) \leq C(data),$$

where C *depends on problem data, but is independent of* h, Δt, *and* γ.

Remark 3.4. *In this case, the term* $\gamma \|\nabla \cdot u_h^n\|^2$ *in estimate* (20) *is* not *identically zero.*

Proof of Lemma 3.2. Unique solvability follows similarly to the proofs in [7, 15]. Unconditional stability follows almost exactly as the proof of Lemma 3.1. The only difference is in Step 1, where the polarization identity gives the left hand side term

$$\|u_h^{n+1}\|^2 - \|\bar{u}_h^n\|^2 + \|u_h^{n+1} - \bar{u}_h^n\|^2,$$

while in the case of the coupled (non-projection) scheme there are no bars (projections). The third term plays no role in the proof, and it simply gets dropped since it is positive on the left hand side. Since the bar denotes the L^2 projection, we have that

$$\|u_h^{n+1}\|^2 - \|u_h^n\|^2 \leq \|u_h^{n+1}\|^2 - \|\bar{u}_h^n\|^2,$$

and with this small change the proof will follow the same as for Lemma 3.1. □

We do not prove convergence of the penalty-projection scheme with respect to h and Δt, although for any fixed $\gamma > 0$, we do expect the reduction in temporal accuracy that projection methods usually produce, *i.e.*, a reduction to $O(\Delta t^{1/2})$ accuracy with respect to the time step size. We do not foresee any major difficulties with combining the convergence analysis of the coupled scheme from [7] with the usual projection method analysis techniques [12, 29, 31] to obtain such a result, but these details need to be worked out before stating them as facts.

Instead, we prove a different kind of convergence, that is perhaps more relevant to the CHNS system. We will prove that for a fixed discretization (*i.e.*, fixed mesh and Δt) and for certain discretizations of velocity-pressure spaces (such as Scott-Vogeliue elements, which as we discuss above are natural for this problem), as $\gamma \to \infty$, the sequence of solutions produced by Algorithm 3.2 will converge to the solution of Algorithm 3.1. In practice this will mean that for γ sufficiently large, the penalty-projection method and coupled method solutions will be very close to identical. In our tests, even with $\gamma = 10$, there is very little difference between the solutions. Hence, in a sense, one can achieve projection method efficiency and coupled method accuracy. Such a result has been proven for Navier-Stokes schemes in [23], and here we extend the ideas to CHNS system.

For the convergence result that follows, we will assume that Scott-Vogelius velocity-pressure elements are used, *i.e.*, $X_h = X \cap [P_k]^d$ and $Q_h = Q \cap P_{k-1}^{\diamond}$. This choice will provide for strongly divergence-free solutions of the coupled scheme, and the Step 2 solution in the penalty-projection scheme. For this element choice to be LBB stable, macro-element mesh structures are required for low order elements; for example, if $k = d$, then a barycenter refinement of a quasi-uniform triangulation is a sufficient criteria on the mesh.

To prove this convergence result, we need to assume additional regularity of the discrete coupled method solution:

$$\max_{1\le n\le L} [\|\hat{u}_h^n\|_{L^\infty} + \|\nabla \hat{u}_h^n\|_{L^3} + \|\hat{\mu}_h^n\|_{H^1}] + \Delta t \sum_{n=1}^{L} \|\hat{p}_h^n\|^2 \le C, \tag{21}$$

with C independent of h and Δt (and of course γ since no grad-div stabilization is used in the coupled scheme). As discussed in [23], due to the convergence result for the coupled scheme, such an assumption is essentially an assumption on the regularity of the true CHNS system solution, and that h and Δt are chosen sufficiently small.

Theorem 3.1. *For a given set of problem data, mesh, time step $\Delta t > 0$, and grad-div stabilization parameter $\gamma \ge 0$, let $(\hat{\phi}_h^{n+1}, \hat{\mu}_h^{n+1}, \hat{u}_h^{n+1}, \hat{p}_h^{n+1}) \in (S_h, S_h, X_h, Q_h)$ be the solution to Algorithm 3.1 (the coupled scheme), and $(\phi_h^{n+1}, \mu_h^{n+1}, u_h^{n+1}, p_h^{n+1}) \in (S_h, S_h, X_h, Q_h)$ be the solution of Algorithm 3.2 (the penalty-projection scheme). Further assuming that (X_h, Q_h) is a Scott-Vogelius element pair, so that $\nabla \cdot X_h \subset Q_h$, and that the coupled method solution is sufficiently regular so that* (21) *holds, the difference in the solutions satisfies*

$$\|\nabla(\phi_h^L - \hat{\phi}_h^L)\| + \|u_h^L - \hat{u}_h^L\| + \left(\Delta t \sum_{n=1}^{L} (\|\nabla(u_h^n - \hat{u}_h^n)\|^2 + \|\nabla(\mu_h^n - \hat{\mu}_h^n)\|^2)\right)^{1/2} \le C(1 + \Delta t^{-1/2})\gamma^{-1}, \tag{22}$$

with C independent of h, Δt, and γ. Thus on a fixed discretization, we expect first order convergence of the penalty-projection scheme to the coupled scheme, as $\gamma \to \infty$.

Remark 3.1. *The negative scaling with respect to Δt does not appear to be removable when obtaining the scaling with γ^{-1}, although we do obtain a bound in* (37) *in the proof which is independent of Δt, but with scaling $\gamma^{-1/2}$. We note that this negative scaling with respect to Δt was also present in a related result for Navier-Stokes schemes in* [23]*, and a mild negative scaling with Δt was observed in their computations. Hence we do not expect to be able to eliminate such a scaling in this case. However, if the Navier-Stokes nonlinear term is removed, then the analysis is likely improvable so that the negative scaling in Δt can be removed entirely.*

Remark 3.2. *The condition number of the penalty-projection scheme will be large if γ is large, and will tend to ∞ as γ does, since the matrix produced by the grad-div term is singular. In our tests, $\gamma = 10^4$ essentially yields numerical convergence, and so we did not take γ larger than this.*

Proof of Theorem 3.1. Throughout the proof, C will represent a generic positive constant independent of $h, \Delta t, \gamma$, and ν (but not ε). Denote

$$\begin{aligned} e^n &= u_h^n - \hat{u}_h^n \in X_h, \quad \text{not necessarily in } V_h, \\ \bar{e}^n &= \bar{u}_h^n - \hat{u}_h^n \in Y_h, \\ e_\phi^n &= \phi_h^n - \hat{\phi}_h^n \in S_h, \\ e_\mu^n &= \mu_h^n - \hat{\mu}_h^n \in S_h. \end{aligned}$$

Begin by subtracting the coupled scheme from the penalty-projection scheme. From our assumption of Scott-Vogelius elements, $\nabla \cdot X_h \subset \nabla \cdot Y_h \subset Q_h$, which implies that $\|\nabla \cdot \hat{u}_h^n\| = \|\nabla \cdot \bar{u}_h^n\| = \|\nabla \cdot \bar{e}^n\| = 0$. This provides the system of equations, for all $(\chi_h, \psi_h, v_h) \in (S_h, S_h, X_h)$,

$$\begin{aligned} &\frac{1}{\Delta t}\left(e_\phi^{n+1} - e_\phi^n, \chi_h\right) \\ &\qquad + B_2(e_\phi^n, \hat{u}_h^{n+1}, \chi_h) + B_2(\phi_h^n, e^{n+1}, \chi_h) + (\nabla e_\mu^{n+1}, \nabla \chi_h) &= 0, \qquad (23) \\ &(e_\mu^{n+1}, \psi_h) - ((\hat{\phi}_h^{n+1})^3 - (\phi_h^{n+1})^3, \psi_h) + (e_\phi^n, \psi_h) \\ &\qquad - \epsilon^2(\nabla e_\phi^{n+1}, \nabla \psi_h) &= 0, \qquad (24) \\ &\frac{1}{\Delta t}(e^{n+1} - \bar{e}^n, v_h) + \gamma(\nabla \cdot e^{n+1}, \nabla \cdot v_h) + \nu(\nabla e^{n+1}, \nabla v_h) \\ &\quad - (\hat{p}_h^{n+1}, \nabla \cdot v_h) + B_0(e^n, \hat{u}_h^{n+1}, v_h) + B_0(u_h^n, e^{n+1}, v_h) \\ &\qquad - \frac{\epsilon^{-1}}{\mathrm{We}} B_2(e_\phi^n, v_h, \hat{\mu}_h^{n+1}) - \frac{\epsilon^{-1}}{\mathrm{We}} B_2(\phi_h^n, v_h, e_\mu^{n+1}) &= 0. \qquad (25) \end{aligned}$$

Step 1: $\Delta t \sum_{n=1}^{L} \|\nabla \cdot e^n\|^2 \leq C\gamma^{-2}$, where C is independent of γ, h and Δt.

Let $\chi_h = \Delta t e_\mu^{n+1}, \psi_h = e_\phi^{n+1} - e_\phi^n, v_h = e^{n+1}$ in (23)-(25). This gives

$$\begin{aligned}
\left(e_\phi^{n+1} - e_\phi^n, e_\mu^{n+1}\right) + \Delta t B_2(e_\phi^n, \hat{u}_h^{n+1}, e_\mu^{n+1}) + \Delta t B_2(\phi_h^n, e^{n+1}, e_\mu^{n+1}) \\
+\Delta t\|\nabla e_\mu^{n+1}\|^2 &= 0, \\
-(\hat{e}_\mu^{n+1}, e_\phi^{n+1} - e_\phi^n) + ((\hat{\phi}_h^{n+1})^3 - (\phi_h^{n+1})^3, e_\phi^{n+1} - e_\phi^n) - \left(e_\phi^{n+1} - e_\phi^n, e_\phi^n\right) \\
+\frac{\epsilon^2}{2}\left(\|\nabla e_\phi^{n+1}\|^2 - \|\nabla e_\phi^n\|^2 + \|\nabla(e_\phi^{n+1} - e_\phi^n)\|^2\right) &= 0, \\
\frac{1}{2\Delta t}\left(\|e^{n+1}\|^2 - \|\bar{e}^n\|^2 + \|e^{n+1} - \bar{e}^n\|^2\right) + \gamma\|\nabla \cdot e^{n+1}\|^2 \\
+\nu\|\nabla e^{n+1}\|^2 - (\hat{p}_h^{n+1}, \nabla \cdot e^{n+1}) + B_0(e^n, \hat{u}_h^{n+1}, e^{n+1}) \\
-\frac{\epsilon^{-1}}{\mathrm{We}} B_2(e_\phi^n, e^{n+1}, \hat{\mu}_h^{n+1}) - \frac{\epsilon^{-1}}{\mathrm{We}} B_2(\phi_h^n, e^{n+1}, e_\mu^{n+1}) &= 0.
\end{aligned}$$

Multiplying the last equation by $\epsilon\mathrm{We}\Delta t$, and then adding the three equations gives

$$\begin{aligned}
&\frac{\epsilon^2}{2}\left(\|\nabla e_\phi^{n+1}\|^2 - \|\nabla e_\phi^n\|^2 + \|\nabla(e_\phi^{n+1} - e_\phi^n)\|^2\right) \\
&\quad + \frac{\epsilon\mathrm{We}}{2}\left(\|e^{n+1}\|^2 - \|\bar{e}^n\|^2 + \|e^{n+1} - \bar{e}^n\|^2\right) + \gamma\epsilon\mathrm{We}\Delta t\|\nabla \cdot e^{n+1}\|^2 \\
&\quad + \nu\epsilon\mathrm{We}\Delta t\|\nabla e^{n+1}\|^2 + \Delta t\|\nabla \hat{e}_\mu^{n+1}\|^2 = -\epsilon\mathrm{We}\Delta t B_0(e^n, \hat{u}_h^{n+1}, e^{n+1}) \\
&\quad + \Delta t B_2(e_\phi^n, e^{n+1}, \hat{\mu}_h^{n+1}) + \left(e_\phi^{n+1} - e_\phi^n, e_\phi^n\right) - \Delta t B_2(e_\phi^n, \hat{u}_h^{n+1}, e_\mu^{n+1}) \\
&\quad + \Delta t(\hat{p}_h^{n+1}, \nabla \cdot e^{n+1}) - ((\hat{\phi}_h^{n+1})^3 - (\phi_h^{n+1})^3, e_\phi^{n+1} - e_\phi^n).
\end{aligned} \tag{26}$$

We now bound the terms on the right hand side. For the first term, Hölder, Sobolev, and Young inequalities, along with assumptions on the true velocity solution of the coupled system, produces

$$\begin{aligned}
\epsilon\mathrm{We}\Delta t|B_0(e^n, \hat{u}_h^{n+1}, e^{n+1})| &\leq C\epsilon\mathrm{We}\Delta t\|e^n\|\left(\|\hat{u}_h^{n+1}\|_{L^\infty} + \|\nabla \hat{u}_h^{n+1}\|_{L^3}\right)\|\nabla e^{n+1}\| \\
&\leq C\epsilon\mathrm{We}\Delta t\nu^{-1}\|e^n\|^2 + \frac{\nu\epsilon\mathrm{We}\Delta t}{8}\|\nabla e^{n+1}\|^2.
\end{aligned}$$

Similarly for the second right hand side term, (since $e^{n+1} \notin V_h$)

$$\begin{aligned}
\Delta t B_2|(e_\phi^n, e^{n+1}, \hat{\mu}_h^{n+1})| &\leq C\Delta t\|\nabla e_\phi^n\| \cdot \|\nabla e^{n+1}\| \cdot \|\hat{\mu}_h^{n+1}\|_{H^1} \\
&\leq C\frac{1}{\epsilon\mathrm{We}}\nu^{-1}\Delta t\|\nabla e_\phi^n\|^2 + \frac{\nu\epsilon\mathrm{We}\Delta t}{8}\|\nabla e^{n+1}\|^2.
\end{aligned}$$

The third term on the right hand side requires some extra work. We first use the dual norm on the time difference, which gives

$$\left(e_\phi^{n+1} - e_\phi^n, e_\phi^n\right) \leq C\Delta t\left\|\frac{e_\phi^{n+1} - e_\phi^n}{\Delta t}\right\|_{-1,h}\|\nabla e_\phi^n\|. \tag{27}$$

Next we need to bound the norm on the time difference in (27). Dividing (23) by $\|\nabla\chi_h\|$ and taking the supremum over all nonzero $\chi_h \in S_h$ yields

$$\begin{aligned}
&\left\|\frac{e_\phi^{n+1} - e_\phi^n}{\Delta t}\right\|_{-1,h} \\
&\leq C\|\nabla \hat{u}_h^{n+1}\| \cdot \left\|\nabla e_\phi^n\right\| + C\|\nabla e^{n+1}\| \cdot \|\nabla \phi_h^n\| + \|\nabla e_\mu^{n+1}\|.
\end{aligned} \tag{28}$$

Combining this with (27) provides the estimate

$$\begin{aligned}\left(e_\phi^{n+1}-e_\phi^n,e_\phi^n\right) &\leq C\Delta t\left(\left\|\nabla e_\phi^n\right\|+\|\nabla e^{n+1}\|+\|\nabla e_\mu^{n+1}\|\right)\|\nabla e_\phi^n\|\\ &\leq \frac{\nu\epsilon\mathrm{We}\Delta t}{8}\|\nabla e^{n+1}\|^2+\frac{\Delta t}{4}\|\nabla e_\mu^{n+1}\|^2\\ &\quad +C\Delta t\left(\frac{1}{\nu\epsilon\mathrm{We}}+1\right)\|\nabla e_\phi^n\|^2. \end{aligned}\tag{29}$$

For the fourth term in (26), we again use Hölder and Sobolev inequalities to find

$$\begin{aligned}\Delta t B_2(e_\phi^n,\hat{u}_h^{n+1},e_\mu^{n+1}) &\leq C\Delta t\|\nabla e_\phi^n\|\cdot\|\nabla\hat{u}_h^{n+1}\|\cdot\|\nabla e_\mu^{n+1}\|\\ &\leq \frac{\Delta t}{4}\|\nabla e_\mu^{n+1}\|^2+C\Delta t\|\nabla e_\phi^n\|^2.\end{aligned}$$

For the pressure term, Cauchy-Schwarz and Young's inequalities provide the bound

$$\Delta t|(\hat{p}_h^{n+1},\nabla\cdot e^{n+1})|\leq\frac{\gamma\epsilon\mathrm{We}\Delta t}{2}\|\nabla\cdot e^{n+1}\|^2+\frac{\Delta t}{2\gamma\epsilon\mathrm{We}}\|\hat{p}_h^{n+1}\|^2.$$

Finally, for the last term in (26), we proceed by first using the operator norm of the time difference,

$$\left|((\hat{\phi}_h^{n+1})^3-(\phi_h^{n+1})^3,e_\phi^{n+1}-e_\phi^n)\right|\leq C\Delta t\left\|\nabla\left((\hat{\phi}_h^{n+1})^3-(\phi_h^{n+1})^3\right)\right\|\cdot\left\|\frac{e_\phi^{n+1}-e_\phi^n}{\Delta t}\right\|_{-1,h},\tag{30}$$

and then using the *a priori* stabilities of $\hat{\phi}_h$ and ϕ_h from Lemmas 3.1 and 3.2

$$\begin{aligned}&\left\|\nabla\left((\hat{\phi}_h^{n+1})^3-(\phi_h^{n+1})^3\right)\right\| \qquad (31)\\ &\leq 3\left(\left\|\phi_h^{n+1}\right\|_{L^\infty}^2+C\left\|\nabla\hat{\phi}_h^{n+1}\right\|_{L^6}\left\|\hat{\phi}_h^{n+1}+\phi_h^{n+1}\right\|_{H^1}\right)\left\|\nabla e_\phi^{n+1}\right\|\\ &\leq C\left\|\nabla e_\phi^{n+1}\right\|. \qquad (32)\end{aligned}$$

Combining this with (28), we obtain

$$\begin{aligned}&\left|((\hat{\phi}_h^{n+1})^3-(\phi_h^{n+1})^3,e_\phi^{n+1}-e_\phi^n)\right|\\ \leq\ & C\Delta t\|\nabla e_\phi^{n+1}\|\left(\left\|\nabla e_\phi^n\right\|+\|\nabla e^{n+1}\|+\|\nabla e_\mu^{n+1}\|\right)\\ \leq\ & \frac{\nu\epsilon\mathrm{We}\Delta t}{8}\|\nabla e^{n+1}\|^2+\frac{\Delta t}{4}\|\nabla e_\mu^{n+1}\|^2\\ &+C\Delta t\left(\frac{1}{\nu\epsilon\mathrm{We}}+1\right)\|\nabla e_\phi^{n+1}\|^2+C\Delta t\|\nabla e_\phi^n\|^2.\end{aligned}$$

Combining the bounds above and using them in (26) yields

$$\begin{aligned}&\frac{\epsilon^2}{2}\left(\|\nabla e_\phi^{n+1}\|^2-\|\nabla e_\phi^n\|^2+\|\nabla(e_\phi^{n+1}-e_\phi^n)\|^2\right)+ \qquad (33)\\ &\frac{\epsilon\mathrm{We}}{2}\left(\|e^{n+1}\|^2-\|\bar{e}^n\|^2+\|e^{n+1}-\bar{e}^n\|^2\right)\\ &+\frac{\gamma\epsilon\mathrm{We}}{2}\Delta t\|\nabla\cdot e^{n+1}\|^2+\frac{\nu\epsilon\mathrm{We}}{2}\Delta t\|\nabla e^{n+1}\|^2+\frac{\Delta t}{4}\|\nabla e_\mu^{n+1}\|^2\\ =&C\epsilon\mathrm{We}\Delta t\nu^{-1}\|e^n\|^2+C\Delta t\left(\frac{1}{\nu\epsilon\mathrm{We}}+1\right)\|\nabla e_\phi^n\|^2\\ &+C\Delta t\left(\frac{1}{\nu\epsilon\mathrm{We}}+1\right)\|\nabla e_\phi^{n+1}\|^2+\frac{\Delta t}{2\gamma\epsilon\mathrm{We}}\|\hat{p}_h^{n+1}\|^2.\end{aligned}$$

Dropping the first order difference terms on the left hand side, noting that $\|\bar{e}^n\| \leq \|e^n\|$ and the $n = 0$ differences are 0, and summing over time steps provides the estimate

$$\begin{aligned}(34)\quad \epsilon^2\|\nabla e_\phi^L\|^2 + \epsilon\mathrm{We}\|e^L\|^2 + \gamma\epsilon\mathrm{We}\ \Delta t\sum_{n=1}^{L}\|\nabla\cdot e^n\|^2 \\ + \nu\epsilon\mathrm{We}\ \Delta t\sum_{n=1}^{L}\|\nabla e^n\|^2 + \Delta t\sum_{n=1}^{L}\|\nabla e_\mu^n\|^2 \\ \leq C\epsilon\mathrm{We}\Delta t\nu^{-1}\|e^n\|^2 + C\Delta t\left(\frac{1}{\nu\epsilon\mathrm{We}}+1\right)\sum_{n=1}^{L}\|\nabla e_\phi^n\|^2 + \frac{\Delta t}{2\gamma\epsilon\mathrm{We}}\sum_{n=1}^{L}\|\hat{p}_h^n\|^2.\end{aligned}$$

Thanks to the Gronwall inequality, we have for Δt sufficiently small that

$$\begin{aligned}(35)\quad \epsilon^2\|\nabla e_\phi^L\|^2 + \epsilon\mathrm{We}\|e^L\|^2 + \gamma\epsilon\mathrm{We}\ \Delta t\sum_{n=1}^{L}\|\nabla\cdot e^n\|^2 \\ + \nu\epsilon\mathrm{We}\ \Delta t\sum_{n=1}^{L}\|\nabla e^n\|^2 + \Delta t\sum_{n=1}^{L}\|\nabla e_\mu^n\|^2 \\ \leq C\gamma^{-1}\Delta t\sum_{n=1}^{L}\|\hat{p}_h^n\|^2,\end{aligned}$$

where C is a constant depending only on problem data, and it independent of γ, h, and Δt. To finish the proof of claim 1, we drop all terms on the left and side except the third one, and use that the pressure term is assumed to be bounded, which yields

$$(36)\qquad \Delta t\sum_{n=1}^{L}\|\nabla\cdot e^n\|^2 \leq C\gamma^{-2}.$$

Note that we also have the bound

$$(37)\qquad \|\nabla e_\phi^L\|^2 + \|e^L\|^2 + \Delta t\sum_{n=1}^{L}\|\nabla e^n\|^2 + \Delta t\sum_{n=1}^{L}\|\nabla e_\mu^n\|^2 \leq C\gamma^{-1},$$

which is less than the scaling predicted the theorem, but with C independent of h, Δt, and γ.

Step 2: $\Delta t\sum_{n=1}^{L}\|\nabla e^n\|^2 \leq \mathcal{O}(\gamma^{-2})$ and $\Delta t\sum_{n=1}^{L}\|\nabla e_\mu^n\|^2 \leq \mathcal{O}(\gamma^{-2})$.

We use the orthogonal decomposition, $X_h = V_h \oplus R_h$, to write $e^n := (e_r)^n + (e_0)^n$, where $(e_r)^n \in R_h$ and $(e_0)^n \in V_h$. From Step 1 and using norm equivalence in R_h, we have that

$$\begin{aligned}\Delta t\sum_{n=1}^{L}\|\nabla(e_r)^n\|^2 \leq& C_R^2\Delta t\sum_{n=1}^{L}\|\nabla\cdot(e_r)^n\|^2 \\ =& C_R^2\Delta t\sum_{n=1}^{L}\|\nabla\cdot e^n\|^2 \leq CC_R^2\gamma^{-2}.\end{aligned}\qquad(38)$$

Since

$$\Delta t \sum_{n=1}^{L} \|\nabla e^n\|^2 = \Delta t \sum_{n=1}^{L} \|\nabla (e_0)^n\|^2 + \Delta t \sum_{n=1}^{L} \|\nabla (e_r)^n\|^2,$$

because to the orthogonal decomposition, we have left to bound only $\Delta t \sum_{n=1}^{L} \|\nabla (e_0)^n\|^2$. We begin this proof similar to Step 1, but we choose a different test function in the momentum equation: $v_h = (e_0)^{n+1}$. This annihilates the pressure and grad-div terms in the momentum equation, and reduces the viscous term due to the orthogonality. Then $\chi_h = \Delta t e_\mu^{n+1}, \psi_h = e_\phi^{n+1} - e_\phi^n, v_h = (e_0)^{n+1}$ in (23)-(25) gives the 3 equations

$$\begin{aligned}
&\left(e_\phi^{n+1} - e_\phi^n, e_\mu^{n+1}\right) \\
&\qquad + \Delta t B_2(e_\phi^n, \hat{u}_h^{n+1}, e_\mu^{n+1}) + \Delta t B_2(\phi_h^n, e^{n+1}, e_\mu^{n+1}) + \Delta t \|\nabla e_\mu^{n+1}\|^2 &&= 0, \\
&-(\hat{e}_\mu^{n+1}, e_\phi^{n+1} - e_\phi^n) + ((\hat{\phi}_h^{n+1})^3 - (\phi_h^{n+1})^3, e_\phi^{n+1} - e_\phi^n) \\
&\qquad - \left(e_\phi^{n+1} - e_\phi^n, e_\phi^n\right) + \frac{\epsilon^2}{2}\left(\|\nabla e_\phi^{n+1}\|^2 - \|\nabla e_\phi^n\|^2 + \|\nabla (e_\phi^{n+1} - e_\phi^n)\|^2\right) &&= 0, \\
&\frac{1}{\Delta t}\left(e^{n+1} - \overline{e}^n, (e_0)^{n+1}\right) + \nu \|\nabla (e_0)^{n+1}\|^2 \\
&\qquad + B_0(u_h^n, e^{n+1}, (e_0)^{n+1}) + B_0(e^n, \hat{u}_h^{n+1}, (e_0)^{n+1}) \\
&\qquad\qquad - \frac{\epsilon^{-1}}{\mathrm{We}} B_2(e_\phi^n, (e_0)^{n+1}, \hat{\mu}_h^{n+1}) - \frac{\epsilon^{-1}}{\mathrm{We}} B_2(\phi_h^n, (e_0)^{n+1}, e_\mu^{n+1}) &&= 0.
\end{aligned}$$

From the skew-symmetry property of B_0, notice that

$$B_0(u_h^n, e^{n+1}, (e_0)^{n+1}) = B_0(u_h^n, (e_r)^{n+1}, (e_0)^{n+1}).$$

For the time derivative term in the momentum equation, we first note that

$$(e^{n+1} - \overline{e}^n, (e_0)^{n+1}) = (e^{n+1} - e^n, (e_0)^{n+1}),$$

which follows from the projection step since $(e_0)^{n+1} \in V_h$. Now we can write

$$\begin{aligned}
\frac{1}{\Delta t}\left(e^{n+1} - e^n, (e_0)^{n+1}\right) &= \frac{1}{\Delta t}\left(e^{n+1} - e^n, e^{n+1}\right) - \frac{1}{\Delta t}\left(e^{n+1} - e^n, (e_r)^{n+1}\right) \\
&= \frac{1}{2\Delta t}\left(\|e^{n+1}\|^2 - \|e^n\|^2 + \|e^{n+1} - e^n\|^2\right) \\
&\quad - \frac{1}{\Delta t}\left(e^{n+1} - e^n, (e_r)^{n+1}\right).
\end{aligned}$$

Multiplying the momentum equation by $\epsilon \mathrm{We} \Delta t$, using the above identities , and then adding the three equations gives

$$\begin{aligned}
&\frac{\epsilon^2}{2}\left(\|\nabla e_\phi^{n+1}\|^2 - \|\nabla e_\phi^n\|^2 + \|\nabla (e_\phi^{n+1} - e_\phi^n)\|^2\right) \\
&+ \frac{\epsilon \mathrm{We}}{2}\left(\|e^{n+1}\|^2 - \|e^n\|^2 + \|e^{n+1} - e^n\|^2\right) + \nu \epsilon \mathrm{We} \Delta t \|\nabla (e_0)^{n+1}\|^2 + \Delta t \|\nabla \hat{e}_\mu^{n+1}\|^2 \\
&\qquad = -\epsilon \mathrm{We} \Delta t B_0(e^n, \hat{u}_h^{n+1}, (e_0)^{n+1}) - \epsilon \mathrm{We} \Delta t B_0(u_h^n, (e_r)^{n+1}, (e_0)^{n+1}) \\
&\qquad + \Delta t B_2(e_\phi^n, (e_0)^{n+1}, \hat{\mu}_h^{n+1}) - \Delta t B_2(\phi_h^n, (e_r)^{n+1}, e_\mu^{n+1}) + \left(e_\phi^{n+1} - e_\phi^n, e_\phi^n\right) \\
&- \Delta t B_2(e_\phi^n, \hat{u}_h^{n+1}, e_\mu^{n+1}) - ((\hat{\phi}_h^{n+1})^3 - (\phi_h^{n+1})^3, e_\phi^{n+1} - e_\phi^n) + \epsilon \mathrm{We}\left(e^{n+1} - e^n, (e_r)^{n+1}\right).
\end{aligned} \tag{39}$$

We now bound the terms on the right hand side. Several of these terms are bounded identical to those of Step 1, but using $(e_0)^{n+1}$ instead of e^{n+1}, and we briefly state

these bounds below. Specifically, for the first, third, fifth, sixth, and seventh terms on the right hand side of (39), we use the bounds

$$\begin{aligned}
\epsilon\mathrm{We}\Delta t|B_0(e^n,\hat{u}_h^{n+1},(e_0)^{n+1})| &\leq C\epsilon\mathrm{We}\Delta t\nu^{-1}\|e^n\|^2+\frac{\nu\epsilon\mathrm{We}\Delta t}{8}\|\nabla(e_0)^{n+1}\|^2,\\
\Delta tB_2|(e_\phi^n,(e_0)^{n+1},\hat{\mu}_h^{n+1})| &\leq C\frac{1}{\epsilon\mathrm{We}}\nu^{-1}\Delta t\|\nabla e_\phi^n\|^2+\frac{\nu\epsilon\mathrm{We}\Delta t}{8}\|\nabla(e_0)^{n+1}\|^2,\\
\left(e_\phi^{n+1}-e_\phi^n,e_\phi^n\right) &\leq \frac{\nu\epsilon\mathrm{We}\Delta t}{8}\|\nabla e^{n+1}\|^2+\frac{\Delta t}{4}\|\nabla e_\mu^{n+1}\|^2\\
&\quad +C\Delta t\left(\frac{1}{\nu\epsilon\mathrm{We}}+1\right)\|\nabla e_\phi^n\|^2,\\
\Delta tB_2(e_\phi^n,\hat{u}_h^{n+1},e_\mu^{n+1}) &\leq \frac{\Delta t}{4}\|\nabla e_\mu^{n+1}\|^2+C\Delta t\|\nabla e_\phi^n\|^2,
\end{aligned}$$

$$\begin{aligned}
&|((\hat{\phi}_h^{n+1})^3-(\phi_h^{n+1})^3,e_\phi^{n+1}-e_\phi^n)|\\
&\quad\leq \frac{\nu\epsilon\mathrm{We}\Delta t}{8}\|\nabla e^{n+1}\|^2+\frac{\Delta t}{4}\|\nabla e_\mu^{n+1}\|^2\\
&\qquad +C\Delta t\left(\frac{1}{\nu\epsilon\mathrm{We}}+1\right)\|\nabla e_\phi^{n+1}\|^2+C\Delta t\|\nabla e_\phi^n\|^2.
\end{aligned}$$

For the second right hand side term, we first add and subtract $\hat{u}_h^n$ in the first argument, then use standard bounds on the B_0 terms to obtain

$$\begin{aligned}
&\epsilon\mathrm{We}\Delta t|B_0(u_h^n,(e_r)^{n+1},(e_0)^{n+1})|\\
&\quad\leq \epsilon\mathrm{We}\Delta t\left(|B_0(\hat{u}_h^n,(e_r)^{n+1},(e_0)^{n+1})|+|B_0(e^n,(e_r)^{n+1},(e_0)^{n+1})|\right)\\
&\quad\leq C\epsilon\mathrm{We}\Delta t\left(\|\nabla\hat{u}_h^n\|\|\nabla(e_r)^{n+1}\|\|\nabla(e_0)^{n+1}\|\right.\\
&\qquad \left.+\|e^n\|^{1/2}\|\nabla e^n\|^{1/2}\|\nabla(e_r)^{n+1}\|\|\nabla(e_0)^{n+1}\|\right)\\
&\quad\leq C\epsilon\mathrm{We}\Delta t\left(C\|\nabla(e_r)^{n+1}\|\|\nabla(e_0)^{n+1}\|+\|\nabla e^n\|^{1/2}\|\nabla(e_r)^{n+1}\|\|\nabla(e_0)^{n+1}\|\right),
\end{aligned}$$

where in the last step we used Lemmas 3.1 and 3.2 and the stability assumption on $\hat{u}_h^n$. Now using Young's inequality provides

$$\begin{aligned}
&\epsilon\mathrm{We}\Delta t\left|B_0(u_h^n,(e_r)^{n+1},(e_0)^{n+1})\right|\\
&\quad\leq \frac{\nu\epsilon\mathrm{We}\Delta t}{8}\|\nabla(e_0)^{n+1}\|^2+C\nu^{-1}\epsilon\mathrm{We}\Delta t\|\nabla(e_r)^{n+1}\|^2\left(1+\|\nabla e^n\|\right)\\
&\quad\leq \frac{\nu\epsilon\mathrm{We}\Delta t}{8}\|\nabla(e_0)^{n+1}\|^2+C\nu^{-1}\epsilon\mathrm{We}\Delta t\|\nabla(e_r)^{n+1}\|^2\left(1+C\Delta t^{-1/2}\gamma^{-1/2}\right),
\end{aligned}$$

with the last step thanks to (37). For the fourth right hand side term of (39), we use the bounds for B_2 from Proposition 2.2, followed by the stability bounds and Young's inequality to obtain

$$\begin{aligned}
\Delta t\left|B_2(\phi_h^n,(e_r)^{n+1},e_\mu^{n+1})\right| &\leq C\Delta t(\|\nabla\phi_h^n\|+|\bar{\phi}|)\|\nabla(e_r)^{n+1}\|\|\nabla e_\mu^{n+1}\|\\
&\leq \frac{\Delta t}{8}\|\nabla e_\mu^{n+1}\|^2+C\Delta t\|\nabla(e_r)^{n+1}\|^2.
\end{aligned}$$

It remains to bound the last right hand side term in (39). Here we utilize Cauchy-Schwarz, Young, and the Poincare inequalities to find that

$$\epsilon\mathrm{We}\left|\left(e^{n+1}-e^n,(e_r)^{n+1}\right)\right| \leq \frac{\epsilon\mathrm{We}}{2}\|e^{n+1}-e^n\|^2+\frac{C^2\epsilon\mathrm{We}}{2}\|\nabla(e_r)^{n+1}\|^2.$$

Combining the above estimates and inserting them in (39) yields

$$\begin{aligned}
&\frac{\epsilon^2}{2}\left(\|\nabla e_\phi^{n+1}\|^2-\|\nabla e_\phi^n\|^2+\|\nabla(e_\phi^{n+1}-e_\phi^n)\|^2\right)+\frac{\epsilon\mathrm{We}}{2}\left(\|e^{n+1}\|^2-\|e^n\|^2\right)\\
&+\frac{\nu\epsilon\mathrm{We}\Delta t}{8}\|\nabla(e_0)^{n+1}\|^2+\frac{\Delta t}{8}\|\nabla e_\mu^{n+1}\|^2\\
\le& C\epsilon\mathrm{We}\Delta t\nu^{-1}\|e^n\|^2+C\nu^{-1}\epsilon\mathrm{We}\Delta t\|\nabla(e_r)^{n+1}\|^2\left(1+C\Delta t^{-1/2}\gamma^{-1/2}\right)\\
&+C\frac{1}{\epsilon\mathrm{We}}\nu^{-1}\Delta t\|\nabla e_\phi^n\|^2+C\Delta t\|\nabla(e_r)^{n+1}\|^2\\
&+\frac{\nu\epsilon\mathrm{We}\Delta t}{8}\|\nabla(e_r)^{n+1}\|^2+C\Delta t\left(\frac{1}{\nu\epsilon\mathrm{We}}+1\right)\|\nabla e_\phi^{n+1}\|^2\\
&+C\Delta t\|\nabla e_\phi^n\|^2+\frac{C^2\epsilon\mathrm{We}}{2}\|\nabla(e_r)^{n+1}\|^2.
\end{aligned}\tag{40}$$

Reducing yields

$$\begin{aligned}
&\epsilon^2\left(\|\nabla e_\phi^{n+1}\|^2-\|\nabla e_\phi^n\|^2\right)+\epsilon\mathrm{We}\left(\|e^{n+1}\|^2-\|e^n\|^2\right)\\
&\qquad+\nu\epsilon\mathrm{We}\Delta t\|\nabla(e_0)^{n+1}\|^2+\Delta t\|\nabla e_\mu^{n+1}\|^2\\
&\qquad\le C\epsilon\mathrm{We}\Delta t\nu^{-1}\|e^n\|^2+C\Delta t\|\nabla e_\phi^n\|^2\\
&\qquad+C\frac{1}{\epsilon\mathrm{We}}\nu^{-1}\Delta t\|\nabla e_\phi^n\|^2+C\Delta t\left(\frac{1}{\nu\epsilon\mathrm{We}}+1\right)\|\nabla e_\phi^{n+1}\|^2\\
&\qquad+C\Delta t\|\nabla(e_r)^{n+1}\|^2\left(1+\nu^{-1}\epsilon\mathrm{We}(1+C\Delta t^{-1/2}\gamma^{-1/2})+\nu\epsilon\mathrm{We}\right)\\
&\qquad\qquad+CC^2\epsilon\mathrm{We}\|\nabla(e_r)^{n+1}\|^2,
\end{aligned}\tag{41}$$

and after summing over time steps, and using that $e^0=0$, $e_\phi^0=0$ and $e_\mu^0=0$, and $\gamma\ge O(1)$, we obtain the bound

$$\begin{aligned}
&\epsilon^2\|\nabla e_\phi^L\|^2+\epsilon\mathrm{We}\|e^L\|^2+\nu\epsilon\mathrm{We}\Delta t\sum_{n=1}^{L}\|\nabla(e_0)^n\|^2+\Delta t\sum_{n=1}^{L}\|\nabla e_\mu^n\|^2\\
&\qquad\le C\epsilon\mathrm{We}\nu^{-1}\Delta t\sum_{n=1}^{L-1}\|e^n\|^2+C\left(1+\frac{1}{\epsilon\mathrm{We}\nu}\right)\Delta t\sum_{n=1}^{L}\|\nabla e_\phi^n\|^2\\
&\qquad+C\left(1+\frac{\epsilon\mathrm{We}}{\nu}+\frac{\epsilon\mathrm{We}\gamma^{-1/2}}{\nu\Delta t^{1/2}}+\frac{\epsilon^{1/2}\mathrm{We}^{1/2}}{\nu}+\nu\epsilon\mathrm{We}\right)\Delta t\sum_{n=1}^{L}\|\nabla(e_r)^n\|^2\\
&\qquad\qquad+\frac{CC^2\epsilon\mathrm{We}}{\Delta t}\Delta t\sum_{n=1}^{L}\|\nabla(e_r)^n\|^2.
\end{aligned}\tag{42}$$

Absorbing the constants into the C's, but with C remaining independent of h, Δt, and γ, and using the bound on $(e_r)^n$ from above, we have that

$$\begin{aligned}
&\|\nabla e_\phi^L\|^2+\|e^L\|^2+\Delta t\sum_{n=1}^{L}\|\nabla(e_0)^n\|^2+\Delta t\sum_{n=1}^{L}\|\nabla e_\mu^n\|^2\le\\
&\qquad C\Delta t\sum_{n=1}^{L-1}\|e^n\|^2+C\Delta t\sum_{n=1}^{L}\|\nabla e_\phi^n\|^2+C\gamma^{-2}\left(1+\Delta t^{-1/2}+\Delta t^{-1}\right).
\end{aligned}\tag{43}$$

TABLE 1. Differences between the divergence-free coupled solution (denoted with hats) and penalty-projection solutions with varying γ. We use the notation $\|\cdot\|_{0,k}$ to denote the $L^2(0,T;H^k(\Omega))$ norm.

γ	$\|\nabla\cdot u_\gamma\|_{0,0}$	rate	S^*	rate	$\|\mu_\gamma-\hat{\mu}\|_{0,1}$	rate	$\|u_\gamma^L-\hat{u}^L\|$	rate	S^{**}	rate
0	9.16e-2	–	2.60e-2	–	5.458e-4	–	1.032e-2	–	8.697e-3	–
1	5.84e-2	–	1.51e-2	–	4.102e-4	–	7.838e-3	–	7.456e-3	–
10	1.92e-2	0.48	5.37e-3	0.45	1.526e-4	0.43	2.875e-3	0.44	3.132e-3	0.38
10^2	2.64e-3	0.86	7.72e-4	0.84	2.174e-5	0.85	4.045e-4	0.85	4.559e-4	0.84
10^3	2.75e-4	0.98	8.09e-5	0.98	2.279e-6	0.98	4.221e-5	0.98	4.778e-5	0.98
10^4	2.76e-5	1.00	8.123e-6	1.00	2.366e-7	0.98	4.239e-6	1.00	4.914e-6	0.99

S^* stands for $\|u_\gamma-\hat{u}\|_{0,1}$ and S^{**} stands for $\|\nabla(\phi_\gamma^L-\hat{\phi}^L)\|$

Now using Gronwall's inequality, assuming Δt is sufficiently small, yields

$$\|\nabla e_\phi^L\|^2+\|e^L\|^2+\Delta t\sum_{n=1}^{L}\|\nabla(e_0)^n\|^2+\Delta t\sum_{n=1}^{L}\|\nabla e_\mu^n\|^2\leq C(1+\Delta t^{-1})\gamma^{-2}. \tag{44}$$

Combining this with the estimate for (e_r) completes the proof.

□

3.3. Numerical convergence of the penalty-projection scheme to the coupled scheme as $\gamma\to\infty$. We now test the predicted convergence rates from Theorem 3.1 for the convergence of the penalty-projection scheme solutions to the coupled scheme solution as $\gamma\to\infty$.

We choose $\Omega=(0,1)^2$ and discretize it uniformly with a $h=1/16$ uniform triangulation, and then apply a barycenter refinement. The element choice is $S_h=P_2$, and Scott-Vogelius velocity-pressure elements $(X_h,Q_h)=(P_2,P_1^\diamond)$, and we note this velocity-pressure pair is stable on this mesh [2]. Initial conditions and parameters are chosen as follows, and we note these parameters come from a test problem in [15]:

$$\Delta t=0.005,\ T=0.05,\ \nu=0.01,\ \epsilon=0.004,\ \mathrm{We}=25, M=1,$$
$$u_0=\langle-\sin(\pi x)^2\sin(2\pi y),\sin(\pi y)^2\sin(2\pi x)\rangle,$$
$$\phi_0=0.24\cos(2\pi x)\cos(2\pi y)+0.4\cos(\pi x)\cos(3\pi y).$$

We note that μ_0 is never needed, as we solve directly for μ_h^{n+1} in the scheme. We impose homogeneous Dirichlet conditions for the velocity u, and homogeneous Neumann conditions for ϕ and μ.

We compute solutions using the coupled scheme, Algorithm 3.1, and the penalty-projection scheme, Algorithm 3.2 using varying γ. The differences between the solutions are shown for each choice of γ in Table 1. First order convergence is observed in u, μ, and ϕ in the appropriate norms, as $\gamma\to\infty$, which verifies the theorem. Observe that with $\gamma=10^4$, the difference between the coupled scheme solution and penalty-projection solution is $O(10^{-6})$ in each of the variables (in these natural norms).

4. Second order schemes for Cahn-Hilliard-Navier-Stokes

In this section, we extend our study to numerical scheme that are second order in time. A coupled scheme second order (Crank-Nicolson) analogue to the first order coupled scheme of the previous section is proposed and studied in [7]. This scheme is proven in [7] to be unconditionally solvable, unconditionally stable, and optimally convergent in space and time. A projection method associated with this coupled scheme is studied in [15], which is more efficient that the coupled scheme, but less

accurate. In this section, we study a relationship between the coupled scheme in [7], and a variant of the projection method of [15] which eliminates the pressure term from the momentum equation and uses grad-div stabilization. After stating the schemes and associated results, we prove that as the grad-div stabilization parameter $\gamma \to \infty$, solutions for the (penalty-)projection scheme converge to the coupled method solution. In effect, this means that with large γ, the (penalty-)projection scheme will produce the same accuracy as the coupled scheme.

4.1. Second order coupled and decoupled schemes for the CHNS system. The second order, Crank-Nicolson type, coupled scheme below is very similar to one studied in [7].

Algorithm 4.1. *(Crank-Nicolson coupled scheme for CHNS system) Given parameters $\epsilon, \mathrm{We}, \nu$, and Δt, find $(\hat{\phi}_h^{n+1}, \hat{\mu}_h^{n+1}, \hat{u}_h^{n+1}, \hat{p}_h^{n+1}) \in (S_h, S_h, X_h, Q_h)$ satisfying for all $(\chi_h, \psi_h, v_h, q_h) \in (S_h, S_h, X_h, Q_h)$,*

$$\begin{aligned}
\frac{1}{\Delta t}\left(\hat{\phi}_h^{n+1} - \hat{\phi}_h^n, \chi_h\right) + B_2(\tilde{\hat{\phi}}_h^{n+1/2}, \hat{u}_h^{n+1/2}, \chi_h) + (\nabla \hat{\mu}_h^{n+1/2}, \nabla \chi_h) &= 0, \\
(\hat{\mu}_h^{n+1/2}, \psi_h) - \frac{1}{2}\left(\left((\hat{\phi}_h^n)^2 + (\hat{\phi}_h^{n+1})^2\right)\hat{\phi}_h^{n+1/2}, \psi_h\right) + (\tilde{\hat{\phi}}_h^{n+1/2}, \psi_h) & \\
-\epsilon^2(\nabla \hat{\phi}_h^{n+1/2}, \nabla \psi_h) &= 0, \\
\frac{1}{\Delta t}(\hat{u}_h^{n+1} - \hat{u}_h^n, v_h) + B_0(\tilde{\hat{u}}_h^{n+1/2}, \hat{u}_h^{n+1/2}, v_h) + \nu(\nabla \hat{u}_h^{n+1/2}, \nabla v_h) & \\
-(\hat{p}_h^{n+1/2}, \nabla \cdot v_h) - \frac{\epsilon^{-1}}{\mathrm{We}} B_2(\tilde{\hat{\phi}}_h^{n+1/2}, v_h, \hat{\mu}_h^{n+1/2}) &= 0, \\
(\nabla \cdot \hat{u}_h^{n+1}, q_h) &= 0,
\end{aligned}$$

where

$$v^{n+1/2} := \frac{v^{n+1} + v^n}{2} \quad \textit{for} \quad v = \hat{u}_h, \hat{\phi}_h,$$

and

$$\tilde{v}^{n+1/2} := \frac{3v^n - v^{n-1}}{2} \quad \textit{for} \quad v = \hat{u}_h, \hat{\phi}_h.$$

Remark 4.1. *Observe that $\hat{\mu}_h^{n+1/2}$ and $\hat{p}_h^{n+1/2}$ are pure variables, whereas $\hat{\phi}_h^{n+1/2}$, $\tilde{\hat{\phi}}_h^{n+1/2}$, $\hat{u}_h^{n+1/2}$ and $\tilde{\hat{u}}_h^{n+1/2}$ are composite.*

We also study a penalty-projection scheme associated with the coupled scheme above. This scheme is similar to that studied in [15], but here we add a grad-div stabilization term to the momentum equation, and remove the pressure from the momentum equation. If no grad-div stabilization is used, then this scheme would be much less accurate that the second order coupled scheme, since pressure is completely removed from the momentum equation. However, we will prove that for large grad-div stabilization parameter γ, solutions found with this scheme will have the same accuracy as the coupled scheme.

Algorithm 4.2. *(2nd-order penalty-projection scheme of CHNS system)*
Step 1: *Find*

$$(\phi_h^{n+1}, \mu_h^{n+1}, u_h^{n+1}) \in (S_h, S_h, X_h)$$

satisfying $\forall(\chi_h,\psi_h,v_h)\in(S_h,S_h,X_h)$

$$\begin{aligned}
\frac{1}{\Delta t}\left(\phi_h^{n+1}-\phi_h^n,\chi_h\right)+B_2(\tilde{\phi}_h^{n+1/2},u_h^{n+1/2},\chi_h)+(\nabla\mu_h^{n+1/2},\nabla\chi_h) &= 0,\\
(\mu_h^{n+1/2},\psi_h)-\frac{1}{2}(\left((\phi_h^n)^2+(\phi_h^{n+1})^2\right)\phi_h^{n+1/2},\psi_h)+(\tilde{\phi}_h^{n+1/2},\psi_h)&\\
-\epsilon^2(\nabla\phi_h^{n+1/2},\nabla\psi_h) &= 0,\\
\frac{1}{\Delta t}(u_h^{n+1}-\bar{u}_h^n,v_h)+\gamma(\nabla\cdot u_h^{n+1/2},\nabla\cdot v_h)+\nu(\nabla u_h^{n+1/2},\nabla v_h)&\\
+B_0(\tilde{u}_h^{n+1/2},u_h^{n+1/2},v_h)-\frac{\epsilon^{-1}}{\mathrm{We}}B_2(\tilde{\phi}_h^{n+1/2},v_h,\mu_h^{n+1/2}) &= 0,
\end{aligned}$$

Step 2: *Find*

$$(\bar{u}_h^{n+1},p_h^{n+1})\in(Y_h,Q_h)$$

such that for every $(v_h,q_h)\in(Y_h,Q_h)$

$$\begin{aligned}
\frac{1}{\Delta t}(\bar{u}_h^{n+1}-u_h^{n+1},v_h)-(p_h^{n+1},\nabla\cdot v_h) &= 0,\\
(\nabla\cdot\bar{u}_h^{n+1},q_h) &= 0.
\end{aligned}$$

where

$$\begin{aligned}
\phi_h^{n+1/2}&=\frac{1}{2}(\phi_h^{n+1}+\phi_h^n),\quad \tilde{\phi}_h^{n+1/2}=\frac{3\phi_h^n-\phi_h^{n-1}}{2},\\
u_h^{n+1/2}&=\frac{1}{2}(u_h^{n+1}+\bar{u}_h^n),\quad \tilde{u}_h^{n+1/2}=\frac{3\bar{u}_h^n-u_h^{n-1}}{2},
\end{aligned}$$

and

$$Y_h\subset Y:=\left\{v\in L^2(\Omega)\;\middle|\;\nabla\cdot v\in L^2(\Omega),\ v\cdot n\,|_{\partial\Omega}=0\right\}.$$

Both schemes above are uniquely solvable and unconditionally energy stable.

Lemma 4.1. *Suppose* $(X_h,Q_h)\subset(X,Q)$ *satisfies the inf-sup condition,* $\nabla\cdot X_h\subset\nabla\cdot Y_h\subset Q_h$*, and* $u_h^0\in V_h$ *and* $\phi_h^0\in S_h$*. Then Algorithm 4.1 is uniquely solvable, and its solution satisfies*

(45)
$$\|\hat{u}_h^L\|^2+\|\nabla\hat{\phi}_h^L\|^2+\Delta t\sum_{n=0}^{L-1}\left(\|\nabla\hat{u}_h^{n+1/2}\|^2+\gamma\|\nabla\cdot\hat{u}_h^{n+1/2}\|^2+\|\hat{\mu}_h^{n+1/2}\|_{H^1}^2\right)\le C(data),$$

where C *depends on problem data, but is independent of* h*,* Δt*, and* γ*. Likewise, Algorithm 4.2 is uniquely solvable, and its solution satisfies*

(46)
$$\|u_h^L\|^2+\|\nabla\phi_h^L\|^2+\Delta t\sum_{n=0}^{L-1}\left(\|\nabla u_h^{n+1/2}\|^2+\gamma\|\nabla\cdot u_h^{n+1/2}\|^2+\|\mu_h^{n+1/2}\|_{H^1}^2\right)\le C(data),$$

where C *depends on problem data, but is independent of* h*,* Δt*, and* γ*.*

4.2. Convergence of the penalty-projection method to the second order coupled scheme. Similar to the first order coupled scheme, we need to assume some additional stability, namely, that there exists a constant C independent of h

and Δt, satisfying

$$\max_{1\le n\le L}\left[\|\hat{u}_h^n\|_{L^\infty}+\|\hat{\phi}_h^n\|_{L^\infty}+\|\phi_h^n\|_{L^\infty}+\|\nabla\hat{u}_h^n\|_{L^3}+\|\hat{\mu}_h^{n-1/2}\|_{H^1}\right] + \Delta t\sum_{n=0}^{L-1}\|\hat{p}_h^{n+1/2}\|^2\le C. \tag{47}$$

Remark 4.2. *It has been shown in the recent paper* [7] *that, using a slightly modified Crank-Nicholson time discretization for the Cahn-Hilliard equation in the coupled scheme (Algorithm 4.1), one can obtain the unconditional stability* $\hat{\phi}_h \in \ell^\infty(0,T;L^\infty(\Omega))$*, as for the first-order-in-time coupled scheme. Using this same treatment in the decoupled scheme, one would expect to obtain* $\phi_h \in \ell^\infty(0,T;L^\infty(\Omega))$*, unconditionally, as well.*

We are now able to state our result for the second order schemes. The proof is very similar to that of the first order schemes, and so we omit it here for brevity.

Theorem 4.1. *For a given set of problem data, mesh, time step* $\Delta t>0$*, and grad-div stabilization parameter* $\gamma\ge 0$*, let* $(\hat{\phi}_h^{n+1},\hat{\mu}_h^{n+1},\hat{u}_h^{n+1},\hat{p}_h^{n+1})\in(S_h,S_h,X_h,Q_h)$ *be the solution to Algorithm 3.2 (the 2nd-order coupled scheme), and* $(\phi_h^{n+1},\mu_h^{n+1},u_h^{n+1},p_h^{n+1})\in(S_h,S_h,X_h,Q_h)$ *be the solution of Algorithm 4.2 (the 2nd-order penalty-projection scheme). Further assuming that* $\nabla\cdot X_h\subset Q_h$*, the difference in the solutions satisfies*

$$\|\nabla(\phi_h^L-\hat{\phi}_h^L)\|+\|u_h^L-\hat{u}_h^L\| + \left(\Delta t\sum_{n=0}^{L-1}(\|\nabla(u_h^{n+1/2}-\hat{u}_h^{n+1/2})\|^2+\|\nabla(\mu_h^{n+1/2}-\hat{\mu}_h^{n+1/2})\|^2)\right)^{1/2}\le C\gamma^{-1}, \tag{48}$$

with C *dependent of* Δt*, but of independent of* h*, and* γ*. Thus on a fixed discretization, we expect first order convergence of the penalty-projection scheme to the coupled scheme, as* $\gamma\to\infty$*.*

4.3. Numerical Experiments for second order schemes. We now give results of three numerical experiments for the second order schemes. Our first experiment illustrates the convergence theorem, and the second experiment tests both the coupled and the penalty-projection schemes on a shape relaxation problem. Our third test is for shape deformation in two phase flow in a lid-driven cavity. In all our tests, we use a Newton iteration to converge the nonlinear problems at each time step.

4.3.1. Numerical Experiment 1: Convergence rate verification. We now test the predicted convergence rates from Theorem 4.1 for the convergence of the penalty-projection scheme solutions to the second order coupled scheme solution as $\gamma\to\infty$. The setup and discretization parameters for this problem are identical to that of the experiment above that verifies Theorem 3.1.

We compute solutions using the second order coupled scheme (Algorithm 4.1), and the penalty-projection scheme (Algorithm 4.2) using varying γ. The differences between the solutions are shown for each choice of γ in Table 2. First order convergence with respect to γ is observed in u, μ, and ϕ in the appropriate norms, as $\gamma\to\infty$, which verifies the theorem.

TABLE 2. Differences between the divergence-free coupled solution (denoted with hats) and penalty-projection solutions with varying γ. We use the notation $\|\cdot\|_{0,k}$ to denote the $l^2(0,T;H^k(\Omega))$ norm.

γ	$\|\nabla\cdot u\|$	rate	$\|u-\hat{u}\|_{0,1}$	rate	$\|\phi-\hat{\phi}\|_{0,1}$	rate	$\|\mu-\hat{\mu}\|_{0,1}$	rate
0	1.612e-01	–	1.968e-02	–	1.103e-04	–	1.504e-04	–
1	2.039e-02	–	7.552e-03	–	9.726e-05	–	6.004e-05	–
10	2.000e-03	1.008	4.194e-03	0.255	7.932e-05	0.089	3.906e-05	0.187
10^2	2.732e-03	-0.136	1.302e-03	0.508	3.098e-05	0.408	1.420e-05	0.440
10^3	5.307e-04	0.712	1.776e-04	0.865	4.153e-06	0.873	1.890e-06	0.876
10^4	5.702e-05	0.969	1.842e-05	0.984	4.291e-07	0.986	1.951e-07	0.986

4.3.2. Numerical experiment 2: Shape relaxation. Our next experiment is for shape relaxation of an isolated shape in a two-phase flow system, and for this test we take $M(\phi) := 0.1\sqrt{(1-\phi)^2+\epsilon^2}$. Even though our analysis assumed $M = 1$, this example suggests that our conclusions should be extendible to a more practical setting. We discretize the domain $\Omega = (0,1)^2$ uniformly with a $h = 1/16$ uniform triangulation, refine around the small square and then apply a barycenter refinement, so that $(P_2, P_1^\diamond)$ Scott-Vogelius elements will be stable [2]. We take $\nu = 0.01, \Delta t = 0.02, \mathrm{We} = 200, \epsilon = 0.005$ and the initial condition to be $u(0,x) = 0$, no-slip velocity boundary conditions, and zero Neumann boundary conditions for ϕ and μ. The initial phase shape is a small square with side length 0.2 located in the middle of a unit square, where we set $\phi_0 = 1$, and we set $\phi_0 = -1$ everywhere else in Ω

We test four schemes for this problem: the coupled scheme using Taylor-Hood elements, the coupled scheme using Scott-Vogelius elements, the penalty-projection scheme (using $(P_2, P_1^\diamond)$ elements for the projection step) with $\gamma = 10^4$, and the projection scheme with (P_2, P_1) Taylor-Hood elements and $\gamma = 0$. The simulation with the $\gamma = 0$ projection scheme failed to give results, as the Newton solver did not converge on the first time step. The other three schemes did produce solutions, and we show plots of their predicted phase fields in Figure 2. Plots are shown at t=0.1, 0.4, and 1.0, and are in good agreement with the known physical solution that the shape will become a circle, since that is the shape that minimizes the free energy [15].

For the three schemes that produced solutions, we also plot their velocity energy $\frac{1}{2}\|u_h\|^2$ with time in Figure 1. Here we observe that the Taylor-Hood coupled solution's velocity energy is more than an order of magnitude larger than the other scheme's solution. This is due to the fact that Taylor-Hood velocity solution will be affected by irrotational forcing of the momentum equation, while the other solutions will not, as they are divergence-free or nearly divergence-free [20]. Once the shape has relaxed to a circle, the forcing of the momentum equation outside of the transition region will be purely potential, and thus will only affect the Taylor-Hood velocity solution.

4.3.3. Numerical experiment 3: 2D Lid driven cavity. Our final experiment is an extension of the previous numerical experiment, but here we prescribe the velocity on the top boundary (the lid) to be $\langle 1, 0\rangle$ instead of no slip, and use $\nu = 0.01$. The corresponds to the well known lid driven cavity problem, except here we again use the same two-phase initial condition as the previous numerical experiment. The rest of the parameters remain the same: $\Delta t = 0.02, \mathrm{We} = 200, \epsilon = 0.005$,

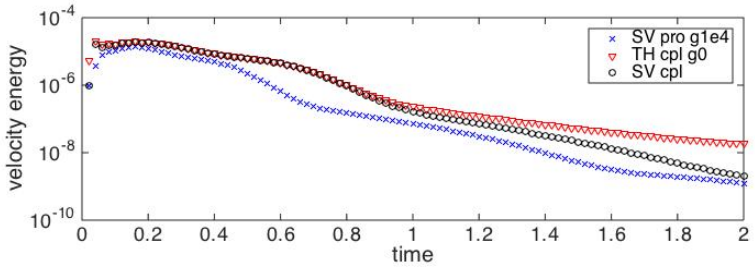

FIGURE 1. Plots of velocity energy $\frac{1}{2}\|u_h\|^2$ with time, for the coupled scheme with Scott-Vogelius (SV) and Taylor-Hood (TH) elements, and the penalty-projection method with $\gamma = 10,000$.

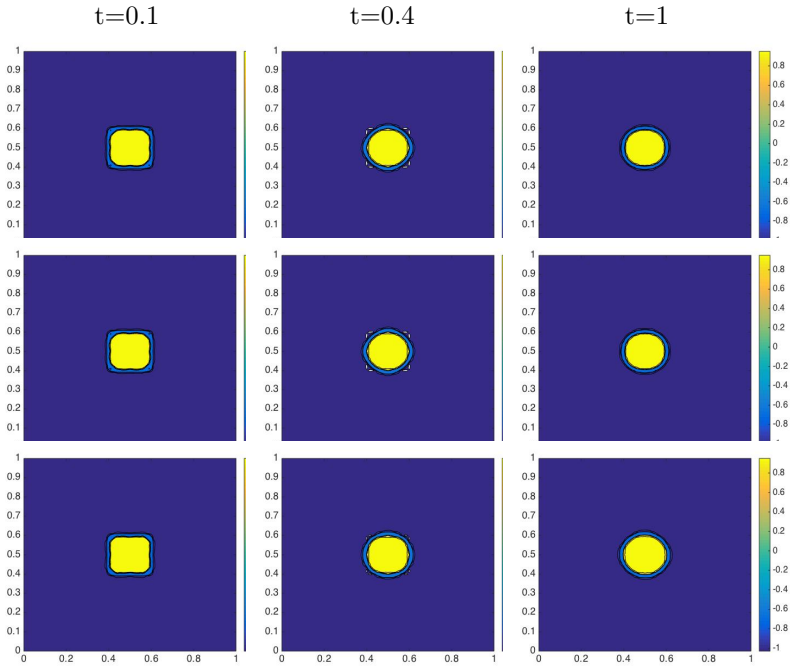

FIGURE 2. Shown above are contour plots of the phase fields for the shape relaxation problem, for the coupled scheme with Scott-Vogelius elements (top), coupled scheme with Taylor-Hood elements (middle), and projection scheme with $\gamma = 10,000$ (bottom).

$M = 0.1\sqrt{(1-\phi)^2 + \epsilon^2}$. The initial velocity is taken to be the Stokes solution for single phase Stokes with $\nu = 0.01$.

We ran simulations with the same 4 schemes as numerical experiment 2, using the same barycenter-refined mesh. Once again, the projection scheme with $\gamma = 0$ failed, as the nonlinear solver did not converge on the first time step. The other three methods converged, and plots of their velocity and phase fields are shows in figure 3. We observe each of the methods give essentially the same prediction of the relaxed shape in the center of the cavity, and that each method's phase field exhibits oscillations at the top boundary. The oscillations in the penalty-projection method

are significantly smaller than that of the coupled methods. The velocity field of the penalty-projection method qualitatively matches that of the single phase Navier-Stokes lid-driven cavity [5], which is expected. However, both coupled schemes have significant oscillations in the velocity at the lid. Thus, it is safe to conclude the penalty-projection scheme does the best job on this problem.

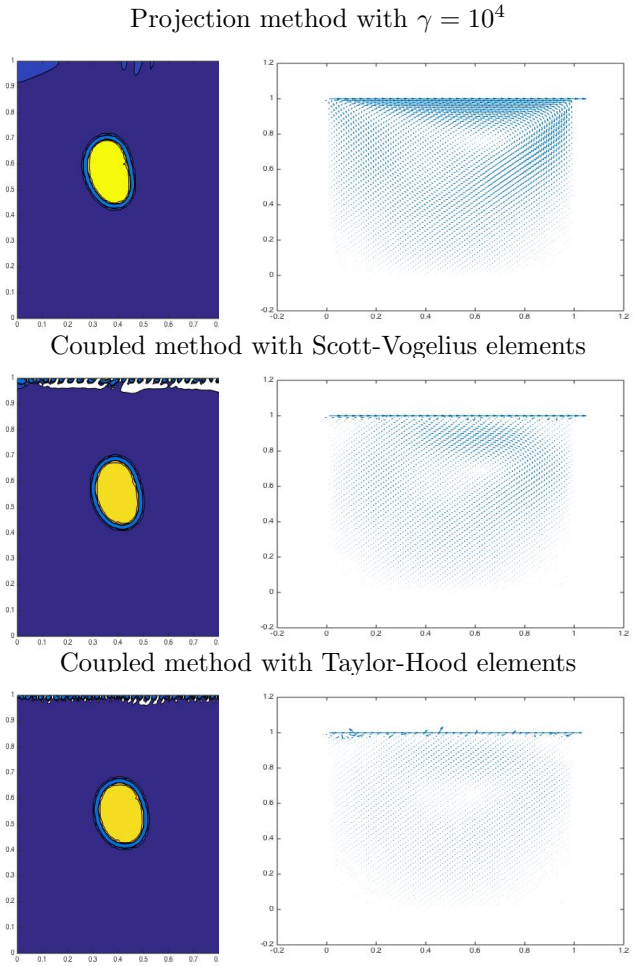

FIGURE 3. Shown above are contour plots of the phase fields for the shape relaxation problem, for the projection scheme with $\gamma = 10,000$ (top), coupled scheme with Scott-Vogelius elements (middle), and coupled scheme with Taylor-Hood elements (bottom).

5. Conclusions

We have established connections between coupled schemes for Cahn-Hilliard-Navier-Stokes and their associated penalty-projection schemes, for both first and second order time stepping schemes. In particular, we proved that in settings where $\nabla \cdot X_h \subset Q_h$ and (X_h, Q_h) is LBB-stable – obtained *e.g.*, using Scott-Vogelius velocity-pressure elements on appropriate meshes – as the penalty parameter $\gamma \to \infty$, the corresponding penalty-projection solutions converge to the

coupled method solution. Thus, in practice, one can use the penalty-projection method with large parameter γ and expect accuracy close to that of the (optimally accurate) coupled scheme. Numerical experiments were given that illustrated the convergence theorems. Additionally, two more numerical experiments were given that tested the penalty-projection method, and showed its effectiveness on problems of physical interest. In fact, for the lid driven cavity shape deformation test problem, the penalty-projection method out-performed the coupled scheme.

For future work, it remains an open problem to study the convergence of the projection method of [15], which is essentially the same as the penalty-projection method of section 4, except without the grad-div stabilization and that the method of [15] includes a lagged pressure term in the momentum equation. Additionally, the development of effective preconditioners for solving the large coupled block linear systems that arise at each time step of both the projection and coupled schemes will be critical for solving large 3D problems.

Acknowledgments

This research was partially supported by NSF grant DMS1522191 and NSF grant DMS1418692.

References

[1] Ph. Angot, M. Jobelin, and J. Latche. Error analysis of the penalty-projection method for the time dependent Stokes equations. *Int. J. Finite Vol.*, 6:1–26, 2009.

[2] D. Arnold and J. Qin. Quadratic velocity/linear pressure Stokes elements. In R. Vichnevetsky, D. Knight, and G. Richter, editors, *Advances in Computer Methods for Partial Differential Equations VII*, pages 28–34. IMACS, 1992.

[3] W. Bangerth, T. Heister, L. Heltai, G. Kanschat, M. Kronbichler, M. Maier, B. Turcksin, and T. D. Young. The `deal.II` library, version 8.2. *Archive of Numerical Software*, 3, 2015.

[4] A. Bowers, S. Le Borne, and L. Rebholz. Error analysis and iterative solvers for Navier-Stokes projection methods with standard and sparse grad-div stabilization. *Computer Methods in Applied Mechanics and Engineering*, 275:1–19, 2014.

[5] B. Cousins, S. Le Borne, A. Linke, L. Rebholz, and Z. Wang. Efficient linear solvers for incompressible flow simulations using Scott-Vogelius finite elements. *Numerical Methods for Partial Differential Equations*, 29:1217–1237, 2013.

[6] A. Diegel, X. Feng, and S.M. Wise. Analysis of a mixed finite element method for a Cahn-Hilliard-Darcy-Stokes system. *SIAM J. Numer. Anal.*, 53:127–152, 2015.

[7] A. Diegel, C. Wang, X. Wang, and S.M. Wise. Convergence analysis and error estimates for a second order accurate finite element method for the Cahn-Hilliard-Navier-Stokes system. *Numer. Math.*, 2017. to appear.

[8] R. Falk and M. Neilan. Stokes complexes and the construction of stable finite elements with pointwise mass conservation. *SIAM J. Numer. Anal.*, 51(2):1308–1326, 2013.

[9] X. Feng and S.M. Wise. Analysis of a Darcy-Cahn-Hilliard diffuse interface model for the Hele-Shaw flow and its fully discrete finite element approximation. *SIAM J. Numer. Anal.*, 50:1320–1343, 2012.

[10] K. Galvin, A. Linke, L. Rebholz, and N. Wilson. Stabilizing poor mass conservation in incompressible flow problems with large irrotational forcing and application to thermal convection. *Computer Methods in Applied Mechanics and Engineering*, 237:166–176, 2012.

[11] V. Girault and P.-A. Raviart. *Finite element methods for Navier–Stokes equations: Theory and algorithms*. Springer-Verlag, 1986.

[12] J. Guermond, P. Minev, and J. Shen. An overview of projection methods for incompressible flows. *Computer Methods in Applied Mechanics and Engineering*, 195:6011–6045, 2006.

[13] J. Guzmán and M. Neilan. Conforming and divergence-free Stokes elements in three dimensions. *IMA Journal of Numerical Analysis*, 34(4):1489–1508, 2014.

[14] J. Guzmán and M. Neilan. Conforming and divergence-free Stokes elements on general triangulations. *Math. Comp.*, 83:15–36, 2014.

[15] D. Han and X. Wang. A second order in time, uniquely solvable, unconditionally stable numerical scheme for Cahn-Hilliard-Navier-Stokes equation. *Journal of Computational Physics*, pages 139–156, 2015.

[16] J. Heywood and R. Rannacher. Finite element approximation of the nonstationary Navier-Stokes problem. Part IV: Error analysis for the second order time discretization. *SIAM J. Numer. Anal.*, 2:353–384, 1990.
[17] J.G. Heywood and R. Rannacher. Finite element approximation of the nonstationary Navier-Stokes problem i: Regularity of solutions and second-order error estimates for spatial discretization. *SIAM J. Numer. Anal.*, 19:275–311, 1982.
[18] E. Jenkins, V. John, A. Linke, and L. Rebholz. On the parameter choice in grad-div stabilization for the stokes equations. *Advances in Computational Mathematics*, 40(2):491–516, 2014.
[19] M. Jobelin, C. Lapuerta, J.-C. Latche, Ph. Angot, and B. Piar. A finite element penalty-projection method for incompressible flows. *Journal of Computational Physics*, 217:502–518, 2006.
[20] V. John, A. Linke, C. Merdon, M. Neilan, and L. Rebholz. On the divergence constraint in mixed finite element methods for incompressible flows. *Submitted*, 2016.
[21] Junseok Kim, Kyungkeun Kang, and John Lowengrub. Conservative multigrid methods for Cahn-Hilliard fluids. *J. Comput. Phys.*, 193(2):511–543, 2004.
[22] A. Linke. On the role of the helmholtz decomposition in mixed methods for incompressible flows and a new variational crime. *Computer Methods in Applied Mechanics and Engineering*, 268:782–800, 2014.
[23] A. Linke, M. Neilan, L. Rebholz, and N. Wilson. A connection between coupled and penalty projection timestepping schemes with FE spatial discretization for the Navier-Stokes equations. *Journal of Numerical Mathematics*, to appear, 2016.
[24] Y. Liu, W. Chen, C. Wang, and S.M. Wise. Error analysis of a mixed finite element method for a Cahn-Hilliard-Hele-Shaw system. *Numer. Math.*, 135:679–709, 2017.
[25] J. Lowengrub and L. Truskinovsky. Quasi-incompressible Cahn-Hilliard fluids and topological transitions. *R. Soc. Lond. Proc. Ser. A Math. Phys. Eng. Sci.*, 454:2617–2654, 1998.
[26] M. Neilan and D. Sap. Stokes elements on cubic meshes yielding divergence-free approximations. *Calcolo*, to appear, 2015.
[27] M. A. Olshanskii. A low order Galerkin finite element method for the Navier-Stokes equations of steady incompressible flow: a stabilization issue and iterative methods. *Comput. Meth. Appl. Mech. Eng.*, 191:55155536, 2002.
[28] M. A. Olshanskii and A. Reusken. Grad-Div stabilization for the Stokes equations. *Math. Comp.*, 73:1699–1718, 2004.
[29] A. Prohl. *Projection and quasi-compressibility methods for solving the incompressible Navier-Stokes equations*. Teubner-Verlag, Stuttgart, 1997.
[30] A. Prohl. On pressure approximation via projection methods for nonstationary incompressible Navier-Stokes equations. *SIAM Journal on Numerical Analysis*, 47(1):158–180, 2008.
[31] J. Shen. On error estimates of some higher order projection and penalty-projection methods for Navier-Stokes equations. *Numerische Mathematik*, 62:49–73, 1992.
[32] S. Zhang. A new family of stable mixed finite elements for the 3d Stokes equations. *Mathematics of Computation*, 74:543–554, 2005.

Department of Mathematical Sciences, Clemson University, Clemson, SC 29634
E-mail: rebholz@clemson.edu
URL: http://www.math.clemson.edu/∼rebholz/

Department of Mathematical Sciences, The University of Tennessee, Knoxville, TN 37996
E-mail: swise1@utk.edu
URL: http://www.math.utk.edu/∼swise/Site/Welcome.html/

Department of Mathematical Sciences, Clemson University, Clemson, SC 29634
E-mail: mengyix@clemson.edu
URL: http://www.math.clemson.edu/∼mengyix/